Phylogenetic analysis of Centralspindlin and Ect2 provides mechanistic insights into the emergence of Metazoa and multicellularity

Michael Glotzer
Molecular Genetics and Cell Biology
University of Chicago
Chicago, IL 60637
mglotzer@uchicago.edu

Abstract

Obligate multicellularity evolved at least 5 times in eukaryotes, including at the origin of Metazoa [1, 2]. However, the molecular events leading to the acquisition of multicellularity are not understood in any lineage. Here, I present an integrated analysis into the contemporaneous emergence of three regulators of cytokinesis and the Metazoan kingdom. Phylogenetic and computational structural analyses indicate that the simultaneous presence of three key regulators of cytokinesis, Kif23, Cyk4, and Ect2 is Metazoan-specific. Structurally, these proteins are highly conserved across all Metazoa. These cytokinetic regulators link the plane of cell division with the position of the spindle during anaphase and subsequently nucleate assembly of stable intercellular bridges [3-6], structures prevalent in Metazoan germlines [7]. Furthermore, certain Choanoflagellates and more basal amoeboid species, some of which exhibit incomplete cytokinesis, encode divergent orthologs of these regulators. These findings, in conjunction with prior knowledge, suggests that evolutionary refinement of these three cytokinetic regulators directly contributed to the evolution of Metazoan multicellularity and germline development.

Results and Discussion

The Metazoan kingdom emerged 650-850 million years ago [8, 9], giving rise to all animals with multicellularity as one of its defining features. Although cell-cell and cell-substrate adhesion play important roles in multicellular organisms, the underlying machinery had evolved extensively in unicellular organisms suggesting that multicellularity did not arise as a direct consequence of the emergence of these functionalities [10]. Furthermore, aggregation-based mechanisms for multicellularity are susceptible to challenges that result from mixing of genetically unrelated cells [11]. An alternative mechanism for multicellularity involves formation of cell clusters that arise from a series of mitoses followed by incomplete cytokineses. This mechanism intrinsically ensures that the functions of a cell cluster are linked to a single genome upon which natural selection can act.

In addition to being multicellular, the last common ancestor of metazoa (LCAM) is inferred to have been a diploid organism that reproduced meiotically via eggs and sperm (anisogamy), as these properties are found in all 5 clades of extant metazoa [7, 12-17]. As first proposed by Zakhvatkin in 1949, an early step in Metazoan evolution was the emergence of the ability to produce gametes and mechanisms to divide fertilized eggs into smaller cells that self-assemble into anisogametic organisms; recent studies have provided additional support to this model [18, 19]. Cytokinesis plays critical roles in many of these processes.

Many of the proteins that promote cytokinesis in Metazoa are evolutionarily ancient [7, 20]. Cleavage furrow ingression in cells from diverse species of Opisthokonts (Metazoa, Fungi, Amoebozoa, etc.) is driven by an actomyosin-based contractile ring assembled from formin-nucleated filamentous actin and non-muscle myosin (Figure 1A). Ring assembly in many

Opisthokonts is triggered by activation of the small GTPase Rho1 through nucleotide exchange [20, 21].

In diverse metazoan species, Ect2 is the guanine nucleotide exchange factor (GEF) that activates Rho1 during cytokinesis (Figure 1A) [22-24]. Ect2 is activated by centralspindlin, a heterotetrameric complex that assembles from dimers of the kinesin-6 family member, Kif23, and Cyk4 (Figure 1B) [25-29]. Association of centralspindlin with the anaphase spindle promotes membrane accumulation of the centralspindlin/Ect2 complex at the cortical region overlying the mid-plane of the spindle, where it promotes local Rho1 activation, contractile ring assembly, and formation of the cleavage furrow [3]. Through this mechanism, the position of the division plane is determined by the position of the spindle during anaphase [24, 30]. Centralspindlin/Ect2 sustains Rho1 activity throughout the furrowing process. Following ingression, centralspindlin nucleates an intercellular bridge that physically connects daughter cells [4-6]. Many, but not all, cells eventually sever this bridge and undergo abscission, generating separate daughter cells [31-35]. Thus, centralspindlin and Ect2 regulate every stage of cytokinesis in animal cells.

To determine the evolutionary history of Kif23, Cyk4, and Ect2, proteins with sequence and domain structure similarity were identified [36-41]. Many proteins, including formin, myosin, and kinases that regulate cytokinesis are widely present in Opisthokonta and more basal lineages (Figure 1C) [20]. In contrast, the full complement of Kif23, Cyk4, and Ect2 is exclusively found in the five metazoan clades (Figure 1C; see below). The overall size and domain structure of these three proteins is highly conserved among extant Metazoa and pairwise sequence identities range from ~30-50% (Figure 1D and Supplemental Figure 1).

The Kif23 subunit of centralspindlin is a kinesin-6 motor protein. The phylogeny of Kif23 indicates that it evolved via duplication of Kif20, a kinesin that contains an extended coiled coil domain (Supplemental Figure 2). Kif23 family members uniquely contain a C-terminal ARF6-binding domain (Figure 1B, Supplementary Figure 3). Whereas Kif20 is present in both Metazoa and Fungi, with one notable exception, Kif23 is Metazoa-specific.

The Cyk4 subunit of centralspindlin is also known as Rac GTPase activating protein 1, MgcRacGAP (mgc:male germ cell), Tumbleweed (*D. melanogaster*), CYK-4 (*C. elegans*). As Cyk4 primarily regulates Rho1 and is not male germ cell specific, the name Cyk4 is used [25, 42]. Cyk4 contains an N-terminal coiled coil followed by a linker region and a C1 domain closely apposed (~25 residues) to the RhoGAP domain (Figure 1B). The unsupervised orthologous group of proteins containing Cyk4 is Metazoan-specific and the domain structure is highly conserved (Supplemental Figure 4, 5).

The interaction between Kif23 and Cyk4 is essential to centralspindlin function [26, 43]. This interaction is mediated by the inter-digitation of two coiled-coil dimers and the N-terminal flanking residues, forming an antiparallel helical bundle [44, 45]. However, the primary sequences of these regions are not highly conserved, beyond the propensity for coiled coil formation. Indeed, mutations that disrupt assembly can be readily suppressed by second site mutations in both cis and trans [26, 43]. To ascertain whether assembly of the centralspindlin complex is conserved throughout Metazoa, predicted structures of the corresponding regions of dimers of Kif23 and Cyk4 from a broad range of Metazoa were generated using Alphafold3 [46]. Cyk4 and Kif23 from species covering all Metazoa phyla folded into similar tetrameric complexes (Figure 2A). These predicted folds closely resemble the experimentally determined structure of *C. elegans* centralspindlin [45]. Thus, centralspindlin complex assembly appears conserved among Metazoa. The Arf6 binding domain at the C-terminus of Kif23 forms a tight dimer of beta sheets and each subunit binds a molecule of active Arf6 [47], presumably at a membrane surface (Figure 2B).

The Rho1 activator, ECT2, contains autoinhibitory tandem BRCT domains [48] (Figure 1B), a Dbl Homology (DH) RhoGEF domain, and a Pleckstrin Homology (PH) domain, though the PH domain is frequently unannotated in many protein domain databases. The BRCT domains of Ect2 associate with Plk1-phosphorylated centralspindlin [49-52], promoting relief from autoinhibition (Figure 1B). The orthologous group containing Ect2 (eggNOG:HUXW8) is populated solely with metazoan proteins (Supplemental Figures 6,7). The additional members of the parental orthologous group (eggNOG:7J7RP) contain a related RhoGEF domain, but these additional proteins lack BRCT domains. Members of the parental orthologous group (eggNOG:7J7RP) contain a related RhoGEF domain, but the additional proteins in this group lack BRCT domains. Structure predictions [53] were used to ascertain the presence of these structural domains in representatives of Ect2 that span Metazoa (Figure 1). In summary, only Metazoan species encode the full set of interaction-competent representatives of Kif23, Cyk4, and Ect2.

The next closest taxonomic clade to Metazoa is Choanoflagellata, followed by Filasteria, and Nucleariids (Figure 3A) [54-56]. Proteins with similarity to Kif23, Cyk4, and Ect2 were identified in the genomes of two Choanoflagellate species, *Salpingoeca rosetta* and *Monosiga brevicollis* MX1 [57] using taxonomically targeted Blast searches using the catalytic domains of Kif23, Cyk4, and Ect2, followed by screening for the presence of the additional domains characteristic of each protein. Both Choanoflagellate species encode two Kif20 kinesins which lack the Arf6 binding domain (Figure 3B). They also encode two paralogous proteins with some structural similarity to Cyk4 and a single Ect2 gene with one or more BRCT domains and a DH domain. The average Alphafold confidence scores (pLDDT) for the BRCT2, BRCT3 and PH domains for *S. rosetta* Ect2 are significantly lower than those of the Metazoan equivalents (Figure Supplement 8). In the case of *M. brevicollis*, the Ect2 ortholog lacks BRCT1 and, like *S. rosetta,* the PH domain has a low confidence score.

To test whether the proteins from *S. rosetta* might be competent to form a centralspindlin-like complex, structural predictions were generated with the four combinations of the two pairs of *S.r.* Cyk4/Kif20 proteins [46]. Only one combination of *S. rosetta* proteins is predicted to form a centralspindlin-like complex with a confidence score > 70 and evidence of an interaction between the two proteins (Figure 3C). The closest ortholog of the *S. rosetta* kinesin that is predicted to form a complex appears truncated in the draft genome of *M. brevicollis* [57], precluding further evaluation. This analysis suggests that centralspindlin-like complexes in Choanoflagellates may have some of the functions of Metazoan centralspindlin, such as microtubule bundling.

The Filasterian species, *Capsaspora owczarzaki,* a unicellular amoeba [58], encodes a kinesin-6 family protein which appears to be a bonafide Kif23 ortholog as it contains an ARF6 binding domain. The closest relative to Cyk4 in *C. owczarzaki* is ~2x longer than Metazoan Cyk4, its C1 and RhoGAP domains are non-adjacent (173 residues), and the coiled coil is far (350 residues) from the N-terminus. The RhoGEF most closely related to Ect2 in *C. owczarzaki* is likewise structurally distinct, as it contains an N-terminal GEF domain and lacks BRCT domains. The Nucleariid social amoeba *Fonticula alba* contains a Kif20 family member (Figure 3B).

The presence of centralspindlin-related proteins in these taxonomic neighbors correlates with the appearance of cytokinetic bridges. *S. rosetta* cells form chains and rosettes via incomplete cell division and ultrastructural analysis reveal electron densities in the intercellular bridge [59, 60]. *Fonticula alba* amoeba generate long bridges whilst dividing [61]. However, a direct role of centralspindlin-related proteins in these events remains to be investigated. Likewise, *Capsaspora* cells form cell aggregates, which can form nonclonally [62]; the potential of preferential clonal aggregation via cell division warrants further analysis.

These observations indicate that proteins with similarity to centralspindlin and Ect2 were variably present in progenitors of Metazoa, Choanoflagellates, and Filasteria and underwent numerous changes prior to the emergence of Metazoa. If centralspindlin-like complexes indeed promote clonal clusters in *S. rosetta* and/or cell bridges in *F. alba*, this would suggest that Kif20/23 and Cyk4 may have first stabilized intercellular bridges and later evolved the ability to interact with Ect2, thereby enabling spindle-dependent control of division plane positioning. Subsequently, the domain structures of these proteins has changed little over the course of ~800 million years (with limited, intriguing exceptions; Supplemental Figure 3). The conservation of protein length and domain organization of Kif23, Cyk4, and Ect2 throughout all clades of Metazoa suggest that, to a first approximation, observations made on extant centralspindlin/Ect2 are a reasonable proxy for the functions of these components in LCAM.

Analysis of extant organisms suggests that the last common ancestor of Ophisthokonta was proficient in mitosis and meiosis and divided using a Rho-regulated contractile array of actomyosin that bisects the elongated anaphase spindle [63]. Given that non-metazoan species were proficient in cytokinesis, what functional consequences might result from the acquisition three additional cytokinetic regulators, Kif23, Cyk4, and Ect2? The mechanism of division plane specification is not conserved amongst Opisthokonts. For example, the division plane of the most studied Fungi, budding and fission yeast, are positioned prior to metaphase, through two distinct mechanisms [64, 65]. Likewise, division plane orientation in Choanoflagellates appears patterned by the position of the flagella [59, 60, 66], though the underlying mechanism(s) are not known. In contrast, centralspindlin and Ect2 are directly implicated in partitioning daughter cells at a position dictated by the mid-plane of the anaphase spindle in a centralspindlin/Ect2 dependent manner [23-26, 30, 67-69]. The linkage of the division plane to the spindle midzone not only prevents aneuploidy, but it also enables regulated spindle displacements to result in asymmetric cell division (Figure 4) and enables the division of cells of vastly different sizes, as the mitotic spindle scales with cell size [70, 71].

In addition, the events at the completion of cytokinesis substantively differ in Metazoa from those that take place in other Opisthokont species. Specifically, as furrowing nears completion, centralspindlin, along with Ect2, accumulates at the center of cytokinetic bridges [23, 25, 68]. This accumulation of centralspindlin bundles the associated microtubules [69] and stabilizes their association with the plasma membrane [72], forming a structure known as the Flemming body, or midbody. Ultimately centralspindlin and Ect2 reorganize into a dense ring at the center of the cytokinetic bridge. A plethora of proteins, not all of which are conserved throughout Metazoa, regulate abscission [7]. While many cells complete abscission, in context-dependent manners, cytokinetic bridges can undergo further maturation and stabilization [73-75], generating stable intercellular bridges.

Stable intercellular bridges constitute a physical connection between related cells, generating a multicellular cluster. Indeed, incomplete cytokinesis suffices to generate a form of clonal multicellularity by partitioning daughter cells without severing/abscising the connections between them. In extant Metazoa, such connections are present in both somatic and germline tissues [76-79] and, where studied, they involve centralspindlin [80]. In *Drosophila* female germlines, centralspindlin templates assembly of ring canals through which materials produced in the nurse cells are delivered into the oocyte as it develops [81, 82]. Functionally analogous structures are present in nematodes and *Hydra* [4, 83]. These structures contribute to fertility, as mutations in centralspindlin and Arf6 can cause sterility [25, 83, 84]. Importantly, such bridges are a conserved feature of germlines across Metazoa [7], suggesting they existed in LCAM (Figure 4).

LCAM was a developmentally complex animal [2, 8]. In addition to the aforementioned roles, centralspindlin/Ect2 could have contributed to generation of developmental complexity in LCAM. By facilitating asymmetric cell division, centralspindlin/Ect2 could enable the specification of distinct cell types [85, 86]. Intercellular trafficking via microtubules of the intercellular bridge regulates cell fate decisions in mouse blastomeres [87]. The Notch pathway, which also emerged at the onset of metazoa [88], can drive binary cell fate decisions, which, in some cases, depends on the spindle midzone [89]. Cytokinetic furrowing and prolonged physical association between daughter cells as a result of delayed abscission can promote cell adhesion between daughter cells [90-93]. More broadly, cell lineages can play a central role in the establishment of developmental complexity [94, 95].

Conceptually, the emergence of Kif23, Cyk4, and Ect2 paired a highly flexible mode of cytoplasmic division with the ability to control the length of time that daughter cells remain physically connected. The ability to prevent completion of cytokinesis itself generates a form of multicellularity. This mechanism intrinsically limits the cell cluster to cells of a common lineage, thereby protecting against genetically distinct cells (cheaters). This protection would be particularly important in the germline, perhaps explaining the remarkable conservation of intercellular bridges at that site [7]. Taken together, the emergence of centralspindlin/Ect2 appears to have been directly involved in the contemporaneous acquisition of several hallmark properties of Metazoa: multicellularity, cell size heterogeneity, and germline development.

Antiparallel microtubules that span nascent daughter cells during telophase are an intrinsic feature of the eukaryotic spindle. Adaptations to these antiparallel microtubules may have contributed to other instances of evolution of multicellularity. Indeed, in green algae, the emergence of incomplete cytokinesis is considered to be one of the earliest steps leading to multicellularity in Volvocine algae [96, 97]. Distinct genetic innovations that modulate the telophase spindle may have contributed to the emergence of multicellularity on multiple occasions during eukaryote evolution.

Acknowledgements

This work was supported by NIH MIRA award 5R35GM127091. MG thanks his lab members past and present and David Pincus, Heather Marlow, Noah Mitchell, and Carlos Cortez (University of Chicago), Marc Kirschner (Harvard Medical School), Pierre Gönczy (ETH, Lausanne), Giacomo Glotzer (Rockefeller University), and Nick Brown (University of Cambridge) for helpful discussions.

Methods

Bioinformatics

Orthologs of Kif23, Cyk4, and Ect2 were identified using a combination of EggNog v.6 [36], OmaDB [37], Uniprot [98], NCBI Blast and NCBI [99].
Domain structures were analyzed using a combination of Conserved Domain Database (CDD) [39], SMART [40], Interpro [41], and Alphafold Structural Database and de novo searches with Alphafold3 [46, 100].

The phylogenetic profile of each unsupervised orthologous group was obtained from EggNog v.6 as were the taxonomic profiles and phylogenetic trees. Clustal Omega was used to generate protein sequence alignments [101].

Centralspindlin complex formation predictions

For each set of putative centralspindlin complexes, the corresponding orthologs of Kif23 and Cyk4 were analyzed with PairCoil2 [102] and the region of putative Cyk4 orthologs from the N-terminus to the end of the coiled coil was paired with the Kif23 sequences ~50 amino acids N-terminus through the end of the coiled coil. These sequences were submitted to Alphafold3 specifying each protein was present in two copies [46]. Predictions were refined by trimming the predicted unstructured termini. If the regions of the proteins were scored with pIDDT > 70, formation of a complex was scored as positive.

Gene predictions

This phylogenetic analysis depends upon gene predictions arising from various genome sequencing projects; many were labeled as “draft” or “preliminary” predictions. During the course of the analysis, some gene annotations appeared questionable and, where possible, revised. Such revisions are justified on the basis of parsimony and an assumption of protein conservation. These issues were particularly necessary for the analysis of species for which there is limited sequence coverage (Ctenophora and Monosiga brevicollis). Sequence coverage of Placazoa and Porifera is also somewhat limited, as Kif23, Cyk4, and Ect2 were not all represented in a single species from these phyla, so representatives from other species were included, as indicated.

Mnemiopsis Cyk4

Data were obtained from the Mnemiopsis Genome Project (the analysis is listed as preliminary). The predicted *Mnemiopsis leidyi* Cyk4 protein was found to be highly similar to the orthologous protein from *Bolinopsis* over much of the body of the protein. However, the predicted N-terminus, which could be involved in the interaction with Kif23, was particularly divergent. Analysis of the genomic sequence revealed a simpler gene model involving fewer and shorter introns, that resulted in far greater identity at the N-terminus with the *Bolinopsis* protein. A predicted transcript from the genomic region (>ML0523.7890.2) resolved the lack of conservation at the C-terminus. This revised prediction was used for the remaining analyses. The alignments of the two versions against the *Bolinopsis* ortholog are appended below.

```
Original
>MNELE06526 | ML05236a | [Mnemiopsis leidyi]
MMFLILSPLTPGQIGVRTTVIPQKYTSHSPIVSGSIQPSTRTGSRTGLRTGLRTGSRTGLAIPEPVREPVRTSYDMITKWIEFISNQADLQQRCHAAEGEVTRLRMQVNQY
KSDKEASDLRVKHIRKQLAEEKSQKQSLSKQNEKLIQQIRVIKEILEDRDRMSMMTDEDKTALGLNRSHLRKQFDKVFEDVSVDLDSDQSLEPSFEGAEELEETKTEWRRR
SRRSNVRKSDRMSTGQVAMKKRRTSNLHAPKEEMEPTTSESSEPPVIYPNLKKFNKANPVPVVAAEVISMSDATTISTTETESDAEYVQSDTESISSTTSESSLPNRAHHF
ALKSMIKPEGCKACRKRLGFSAHALRCKYCKMVVHVECKNAAPMPCVPVLSTSSKKQDGTLGSYVPKNPPHVPSILLRCVQEIEARGLNETGLYRVTGPDKAIKELKERML
RPRCQTNLRKVEDTTILTGVVKNFLMNLNDPILTSALSDEFKEYAEKGSTNHLYGTISKLPHENRHTLAFMIIHLQKVSESEHCKMPRSNIARVFAPTLVASIAMTDMDSA
MRDTKRSAKVVECLLDLPPSYWHNMLNPHDECSSPTPYSHDEAPHTPGTPEMLKGRNFFFLKLFLLTIKHSLTQNDIIDKMLLRSQCRSHLYSYEDCH
revised:
>MNELE06526_revised | ML05236a | [Mnemiopsis leidyi]
```

```
MSRKKSSSRQSLGAVRNTPSAYFDEICQISSILNCGLEQEWIEFISNQADLQQRCHAAEGEVTRLRMQVNQYKSDKEASDLRVKHIRKQLAEEKSQKQSLSKQNEKLIQQI
RVIKEILEDRDRMSMMTDEDKTALGLNRSHLRKQFDKVFEDVSVDLDSDQSLEPSFEGAEELEETKTEWRRRSRRSNVRKSDRMSTGQVAMKKRRTSNLHAPKEEMEPTTS
ESSEPPVIYPNLKKFNKANPVPVVAAEVISMSDATTISTTETESDAEYVQSDTESISSTTSESSLPNRAHHFALKSMIKPEGCKACRKRLGFSAHALRCKYCKMVVHVECK
NAAPMPCVPVLSTSSKKQDGTLGSYVPKNPPHVPSILLRCVQEIEARGLNETGLYRVTGPDKAIKELKERMLRPRCQTNLRKVEDTTILTGVVKNFLMNLNDPILTSALSD
EFKEYAEKGSTNHLYGTISKLPHENRHTLAFMIIHLQKVSESEHCKMPRSNIARVFAPTLVASIAMTDMDSAMRDTKRSAKVVECLLDLPPSYWHNMLNPHDECSSPTPYS
HDEAPHTPGTPEMLKGRNFFFLKLFLLTIKHSLTQNDIIDKMLLRSQCRSHLYSYEDCH

>XP_063677920.1 rac GTPase-activating protein 1-like [Bolinopsis microptera]
MTKKKSTSRQSLGAARNAPSAYFDELCQISTILNCGLEQEWIEFISNQADLQQRCQAAEGEVTRLRVQVN
QFKSDKEASDLRVKHMRKQLAEEKSQKQALSKLNEKLVQQIRVIKEILEDRDRMSMMTDEDKTALGLNKS
HLRKQFDKVFEDVSVDLDSDQSLEPSFEGELEETRTEWRRRSRRSNVRKSERQSTGPGVTVKKRRTSNLH
HPPKEDIYMTMEPTSSESSEPPVIYPNLKKFNKAHPVPHVEAEVISVQSSEATTISTTETESDVDYLPSD
TESISSTTSESSLPNRPHHFALKSMIKPEGCKACRKRLGFSAHALRCKYCKMVVHQDCKNAAPMPCVPIL
STPSRKQDGSLFSYVPKNPPHVPSIMLRCVQEIEARGLNEIGLYRVTGPDKAIKELKERMLRPRCQTNLR
KIDDTTILTGVLKNFLMNLNDPILTSALSDEFKNNAEKGSANHLYGTISKLPHENRHTLAFLIIHLQKVA
ESEHCKMPRSNIARVFAPTLVASIAMTDMDSAMRDTKRSAKVVECLLDLPPYYWTNMLNPHEDCSSPTPY
SNDEAPRTPGTPEMLKVQPGMYQPPTPTNAKETTFTQRVFGGKKKTFFNKFETP
```

```
CLUSTAL O(1.2.4) multiple sequence alignment
```

Alignment of draft Mnemiopsis gene prediction vs Bolinopsis

```
MNELE06526          MMFLILSPLTPGQIGVRTTVIPQKYTSHSPIVSGSIQPSTRTGSRTGLRTGLRTGSRTGL      60
XP_063677920.1      ------------------------------------MTKKKSTSRQSLGAA--RN-APSA      21
                                                          ..:: ** .* :.   .   . 

MNELE06526          AIPEPVREPVRTSYDMITKWIEFISNQADLQQRCHAAEGEVTRLRMQVNQYKSDKEASDL120
XP_063677920.1      YFDELCQISTILNCGLEQEWIEFISNQADLQQRCQAAEGEVTRLRVQVNQFKSDKEASDL81
                     : *  :  .  . .:  :***************:**********:****:*********

MNELE06526          RVKHIRKQLAEEKSQKQSLSKQNEKLIQQIRVIKEILEDRDRMSMMTDEDKTALGLNRSH      180
XP_063677920.1      RVKHMRKQLAEEKSQKQALSKLNEKLVQQIRVIKEILEDRDRMSMMTDEDKTALGLNKSH      141
                    ****:************:*** ****:******************************:**

MNELE06526          LRKQFDKVFEDVSVDLDSDQSLEPSFEGAEELEETKTEWRRRSRRSNVRKSDRMSTGQ-V      239
XP_063677920.1      LRKQFDKVFEDVSVDLDSDQSLEPSFEG--ELEETRTEWRRRSRRSNVRKSERQSTGPGV      199
                    ****************************  *****:***************:* ***  *

MNELE06526          AMKKRRTSNLHAPKE-----EMEPTTSESSEPPVIYPNLKKFNKANPVPVVAAEVISM--      292
XP_063677920.1      TVKKRRTSNLHHPPKEDIYMTMEPTSSESSEPPVIYPNLKKFNKAHPVPHVEAEVISVQS      259
                    ::********* * :      ****:*******************:*** * *****:  

MNELE06526          SDATTISTTETESDAEYVQSDTESISSTTSESSLPNRAHHFALKSMIKPEGCKACRKRLG      352
XP_063677920.1      SEATTISTTETESDVDYLPSDTESISSTTSESSLPNRPHHFALKSMIKPEGCKACRKRLG      319
                    *:************.:*: ****************** **********************

MNELE06526          FSAHALRCKYCKMVVHVECKNAAPMPCVPVLSTSSKKQDGTLGSYVPKNPPHVPSILLRC      412
XP_063677920.1      FSAHALRCKYCKMVVHQDCKNAAPMPCVPILSTPSRKQDGSLFSYVPKNPPHVPSIMLRC      379
                    **************** :***********:*** *:****:* *************:***

MNELE06526          VQEIEARGLNETGLYRVTGPDKAIKELKERMLRPRCQTNLRKVEDTTILTGVVKNFLMNL      472
XP_063677920.1      VQEIEARGLNEIGLYRVTGPDKAIKELKERMLRPRCQTNLRKIDDTTILTGVLKNFLMNL      439
                    *********** ******************************::********:*******

MNELE06526          NDPILTSALSDEFKEYAEKGSTNHLYGTISKLPHENRHTLAFMIIHLQKVSESEHCKMPR      532
XP_063677920.1      NDPILTSALSDEFKNNAEKGSANHLYGTISKLPHENRHTLAFLIIHLQKVAESEHCKMPR      499
                    **************: *****:********************:*******:*********

MNELE06526          SNIARVFAPTLVASIAMTDMDSAMRDTKRSAKVVECLLDLPPSYWHNMLNPHDECSSPTP      592
XP_063677920.1      SNIARVFAPTLVASIAMTDMDSAMRDTKRSAKVVECLLDLPPYYWTNMLNPHEDCSSPTP      559
                    ****************************************** ** ******::******

MNELE06526          YSHDEAPHTPGTPEMLKGRNFFFLKLFLLTIKHSLTQNDIIDKMLLRSQCRSHLYSYEDC      652
XP_063677920.1      YSNDEAPRTPGTPEMLKVQPGMYQPPTPTNAKETTFT-----QRVFGGKKKTFFNKFETP      614
```

```
                    **:****:********* :  ::      . *.:        : :: .: ::.: .:*

MNELE06526          H     653
XP_063677920.1      -     614
```

Alignment of revised Mnemiopsis gene prediction vs Bolinopsis

```
XP_063677920.1           MTKKKSTSRQSLGAARNAPSAYFDELCQISTILNCGLEQEWIEFISNQADLQQRCQAAEG 60
MNELE06526_revised2      MSRKKSSSRQSLGAVRNTPSAYFDEICQISSILNCGLEQEWIEFISNQADLQQRCHAAEG 60
                         *::***:*******.**:*******:****:************************:****

XP_063677920.1           EVTRLRVQVNQFKSDKEASDLRVKHMRKQLAEEKSQKQALSKLNEKLVQQIRVIKEILED 120
MNELE06526_revised2      EVTRLRMQVNQYKSDKEASDLRVKHIRKQLAEEKSQKQSLSKQNEKLIQQIRVIKEILED 120
                         ******:****:*************:************:*** ****:************

XP_063677920.1           RDRMSMMTDEDKTALGLNKSHLRKQFDKVFEDVSVDLDSDQSLEPSFEG--ELEETRTEW 178
MNELE06526_revised2      RDRMSMMTDEDKTALGLNRSHLRKQFDKVFEDVSVDLDSDQSLEPSFEGAEELEETKTEW 180
                         ******************:******************************  *****:***

XP_063677920.1           RRRSRRSNVRKSERQSTGPGVTVKKRRTSNLHHPPKEDIYMTMEPTSSESSEPPVIYPNL 238
MNELE06526_revised2      RRRSRRSNVRKSDRMSTGQ-VAMKKRRTSNLHAPKE-----EMEPTTSESSEPPVIYPNL 234
                         ************:* ***  *::********* * :      ****:*************

XP_063677920.1           KKFNKAHPVPHVEAEVISVQSSEATTISTTETESDVDYLPSDTESISSTTSESSLPNRPH 298
MNELE06526_revised2      KKFNKANPVPVVAAEVISM--SDATTISTTETESDAEYVQSDTESISSTTSESSLPNRAH 292
                         ******:*** * *****:  *:************.:*: ****************** *

XP_063677920.1           HFALKSMIKPEGCKACRKRLGFSAHALRCKYCKMVVHQDCKNAAPMPCVPILSTPSRKQD 358
MNELE06526_revised2      HFALKSMIKPEGCKACRKRLGFSAHALRCKYCKMVVHVECKNAAPMPCVPVLSTSSKKQD 352
                         ************************************* :***********:*** *:***

XP_063677920.1           GSLFSYVPKNPPHVPSIMLRCVQEIEARGLNEIGLYRVTGPDKAIKELKERMLRPRCQTN 418
MNELE06526_revised2      GTLGSYVPKNPPHVPSILLRCVQEIEARGLNETGLYRVTGPDKAIKELKERMLRPRCQTN 412
                         *:* *************:************** ***************************

XP_063677920.1           LRKIDDTTILTGVLKNFLMNLNDPILTSALSDEFKNNAEKGSANHLYGTISKLPHENRHT 478
MNELE06526_revised2      LRKVEDTTILTGVVKNFLMNLNDPILTSALSDEFKEYAEKGSTNHLYGTISKLPHENRHT 472
                         ***::********:*********************: *****:*****************

XP_063677920.1           LAFLIIHLQKVAESEHCKMPRSNIARVFAPTLVASIAMTDMDSAMRDTKRSAKVVECLLD 538
MNELE06526_revised2      LAFMIIHLQKVSESEHCKMPRSNIARVFAPTLVASIAMTDMDSAMRDTKRSAKVVECLLD 532
                         ***:*******:************************************************

XP_063677920.1           LPPYYWTNMLNPHEDCSSPTPYSNDEAPRTPGTPEMLKVQPGMYQPPTPTNAKETTFTQR 598
MNELE06526_revised2      LPPSYWHNMLNPHDECSSPTPYSHDEAPHTPGTPEMLKVQPGMYQPPTPTNSKETTFTQR 592
                         *** ** ******::********:****:**********************:********

XP_063677920.1           VFGGKKKTFFNKFETP  614
MNELE06526_revised2      VFGGKKKTFFNKFETP  608
                         ****************
```

Mnemopsis Ect2 ortholog

The closest annotated ortholog to Ect2 in Mnemiopsis is ML444210a:

```
>ML444210a [from Mnemnopsis genome project]
MYHDRPEDSEMNDFITQLGIENPATLDKSEIGSAVRQYAVLPDFEMGEKFLSKLQARHVRVISPVLIKQCLVSGRPLGSFRRFLMPGRRCYPMFSSMMVGLTIGFTNFPSR
EDLKRMRWMVEVLGGRVTREYDPMGKIILIANMAGRDKFETAMACGEPVLKVDWLNDCYSLRMEPNVLPRLMYAEDNQRYACEIFYRFKFFLIGFKEYDAVDIKENCKRYG
AVVFEEVSVMRKCTHVIIYESSDQSAYQPYLEELRKICSREGDLSTQLVTDKWFYESVSLSALLDTNRYSITISPDGTLDFSSAHDRKRRVDELSADSCPRKKRSSEANCS
IYSNISITGQLPKTPKNTPKTIDKRDNVISEFIRTEETYVRHLKIIEERYYGYLYEQVANPPANNKFELELPSVHMMFQKIVPIRIVHGALLKELERYEVSEKLRKDSKKN
RGEKSFGRILLNWIGKEVFKDENAPDGISFLNYSREEMIKMFQYDKNETRDYLRFDPGRTSSEKRDEGERRRDQEKRRKEYEGTMRKKPSGEVQGEDPDVLKHYNIYMNAH
EGILDLINKNETKCFSEKIEKKLLTLLVKYWVSELQLLVFCNFSLCRERTVTVQENVRQTSNTPGHSRKSGVGTKVYPLGGNVDFCPLRRGSCMCQGAGSELLELPPRTLL
RSGRCTRTCRHSPADTPSPGPRSSSRSRHLGEKSGCRGASIPRT
```

This gene model is likely to be partially mis-annotated. The first ~484 amino acids are highly homologous to Ect2 (the top hit vs C. elegans is ECT-2), but the sequences diverge at that point. The first 270 amino acids are predicted to form ~2+ tandem BRCT domains. However, the DH domain is incomplete and the PH domain is absent. The transcriptomic databases of the Mnemiopsis genome project contains a Trinity assembled transcript (ML4442|comp13217_c0_seq1), that is identical to ML444210a over amino acids 21-561. However, at that point they diverge and the ML4442 transcript encodes a protein that is more similar to ECT2 including a short sequence (PVQR) that is invariant in Ect2 proteins. Thus, here I used a hybrid protein that contains the missing N-terminus of ML4442 from ML444210 and the C-terminus of ML444210A. However, this sequence is still unlikely to be fully accurate, as the underlined sequence is highly divergent and the C-terminus is likely truncated. However, no other source of Ect2 could be found in Ctenophora. Due to the lack of reliable sequences, this Ect2 protein was excluded from the analysis is Supplemental Figure 8.

```
N-Terminus of ML444210a-shared-C-terminus of ML4442|comp13217_c0_seq1

MYHDRPEDSEMNDFITQLGIENPATLDKSEIGSAVRQYAVLPDFEMGEKFLSKLQARHVRVISPVLIKQC
LVSGRPLGSFRRFLMPGRRCYPMFSSMMVGLTIGFTNFPSREDLKRMRWMVEVLGGRVTREYDPMGKIIL
IANMAGRDKFETAMACGEPVLKVDWLNDCYSLRMEPNVLPRLMYAEDNQRYACEIFYRFKFFLIGFKEYD
AVDIKENCKRYGAVVFEEVSVMRKCTHVIIYESSDQSAYQPYLEELRKICSREGDLSTQLVTDKWFYESV
SLSALLDTNRYSITISPDGTLDFSSAHDRKRRVDELSADSCPRKKRSSSEANCSIYSNISITGQLPKTPK
NTPKTIDKRDNVISEFIRTEETYVRHLKIIEERYYGYLYEQVANPPANNKFELELPSVHMMFQKIVPIRI
VHGALLKELERYEVSEKLRKDSKKNRGEKSFGRILLNWIGKEVFKDENAPDGISFLNYSREEMIKMFQYD
KNETRDYLRFDPGRTSSEKRDEGERRRDQEKRRKEYEGTMRKKPSGEVQGEDPDVLKHYNIYMNAHEGIL
DLINKNETKCFRFRSYLRTEGAKKENDRLSIKDLMIEPVQRLPRIILLLDAIIKKTDKKHGDLELLEIVR
EEFKKVTVYVNDSKRKLDQKKEFVNFLMQISGLPEGVISTSKHNLVEQYHFKLYREIGH
```

Monosiga brevicollis Cyk4 paralogs

The Monosiga brevicollis protein MONBRDRAFT_34379 (https://www.ncbi.nlm.nih.gov/gene?cmd=retrieve&list_uids=5895264 ; https://www.ncbi.nlm.nih.gov/protein/XP_001749975.1) derived from the genome sequencing project [57] contains a C1:RhoGAP domain. The first two exons of this predicted protein is replete with repeats of the dipeptides TH (12) and TE (47). These sequences are derived from a predicted exon separated from the remainder of the protein by an intron 289 nt long (188374-188665) which is larger than the average Monosiga brevicollis intron length of 174 nt. The first ATG of this protein is more likely to be at position 188722; this prediction was used for further analysis.

Monosiga brevicollis A9V1W6 (aka XM_001746567.1) is predicted to encode a 1365 aa protein containing a RhoGAP domain at 436-636. Following the RhoGAP domain, in the genomic sequence corresponding to amino acid 657, there is a predicted intron of 530 bp, longer that the average intron size of in this organism of 174 nt. The protein sequence that follows in exon 9 and beyond (listed below) is 35% identical to bacterial proteins containing a DUF6259 domain (e.g. https://www.ebi.ac.uk/interpro/entry/InterPro/IPR046226/alphafold/#table). Based on the protein size, intron length, and unusual homology this draft gene annotation is likely erroneous. Here, the analysis of the protein was limited to the N-terminal RhoGAP domain containing portion.

```
>C-terminus of A9V1W6
KKQNISLLLTLTTPSSLLVLNTDGSIADLRARTANPGNWSFVLDAHRPIFTFLASGVEPTGPTSNISARDCKAWPPELVNATQARVRFLCPSTLVPA
AAFDITVSVQADQERDQFLFGLELNINATNASVVLSALEFPLLTMAAIRDEMLLSEDNIVMPYAGGTRNNMPGIASEAQSQMYPGYASFQFWARSGF
KALKPHRFVILHVKEFVYTSAAHDSINITVRHHRPWIPFDAATPFLPYQTALRTFSGDWMTAATLYKAWAGQQWWTRTPLTRRTDIPSFLLNGTGVW
ISGINSQSGFNPNRWEHDGTWAGIDYLPPQPSADAWQNATQQLLAQSSNGPAFNHTTQMLAHQSMLVRNNDQTLAAVDAYNEPEGPQGWRGYSTRLC
HGSREAQTVLGAIFHQVSALNVSLISFDQEIGGGARYPCYANNHGHALGWGPWMYHEFAQLVQEIKANATHQGIMTEQVSELTIPLMATYWSRQFAQ
```

```
QHYFFFRGYGEPIFNFLYHEFVTTIGAAEVQGQGEVAQYRSVVLRRAVIGDCVARGMLQGPFDSDVSLAPVPGSFSQNISMLFFNISATYSHYAEYV
TLGQMVRPPISRNPVDLTTTLVWKRGNGSFVREAVNTSALRLGAFMAPEGTVGILIVNIDDVTHSVTLDITQTWKPPPNATVMIYDEQCRPMGTAKV
EQSGSTVQLVVPGLRLRFLALSPPSCAQ
```

Monosiga brevicollis Kif23 paralog

One relevant gene from *Monosiga brevicollis* is MONBRDRAFT_13496, (XP_001742878.1). This kinesin is the closest ortholog of *S. Rosetta* kinesin PTSG00966, but it is a partial sequence. The annotation specifies that it is N-terminally truncated. The predicted protein is missing the initiator methionine, but more importantly for these purposes it is missing the parts after the motor domain, which would be the region that could interact with Cyk4.This truncated protein was used in the analysis to the limited extent possible, with the understanding that it is undoubtedly incomplete.

```
>XP_001742878.1 uncharacterized protein MONBRDRAFT_13496, partial [Monosiga brevicollis MX1]
CSLQQVDIEHDDVRYGVFVQYVEIYNNYCYDLLVPPPPEKEPAKPRPPTRQSLKISQDETGHRYVREAIWKEVHTPEEAFELLHQGQITRATAATDL
NATSSRSHSIFTIRLVSAPTSMRGNDVQRDGPTPHVADISLVDLAGSERTSRTNSTGDRRKEAGAINKSLSVLRDCMKALRRNQDNGSRGKPKFNES
SLTKLFERFLTGDGLAAMVVCASPAQSDASETAHVFDFAKVASDVQVEAPVHVMQDHGKLLDHGVRTHTRPACQEQCKPRTFGSFITRLVSFIEWKS
```

References

1. Grosberg R.K., and Strathmann R.R. (2007). The Evolution of Multicellularity: A Minor Major Transition? Annual Review of Ecology, Evolution, and Systematics. 38, 621-654.
2. Knoll A.H. (2011). The Multiple Origins of Complex Multicellularity. Annual Review of Earth and Planetary Sciences. 39, 217-239.
3. Basant A., and Glotzer M. (2018). Spatiotemporal Regulation of RhoA during Cytokinesis. Curr Biol. 28, R570-R580.
4. Price K.L., Tharakan D.M., and Cooley L. (2023). Evolutionarily conserved midbody remodeling precedes ring canal formation during gametogenesis. Dev Cell. S1534-5807(23)00050.
5. Zhou K., Rolls M.M., and Hanna-Rose W. (2013). A postmitotic function and distinct localization mechanism for centralspindlin at a stable intercellular bridge. Dev Biol. 376, 13-22.
6. Greenbaum M.P., Ma L., and Matzuk M.M. (2007). Conversion of midbodies into germ cell intercellular bridges. Dev Biol. 305, 389-396.
7. Chaigne A., and Brunet T. (2022). Incomplete abscission and cytoplasmic bridges in the evolution of eukaryotic multicellularity. Curr Biol. 32, R385-R397.
8. Erwin D.H., Laflamme M., Tweedt S.M., Sperling E.A., Pisani D., and Peterson K.J. (2011). The Cambrian conundrum: early divergence and later ecological success in the early history of animals. Science. 334, 1091-1097.
9. dos Reis M., Thawornwattana Y., Angelis K., Telford M.J., Donoghue P.C., and Yang Z. (2015). Uncertainty in the Timing of Origin of Animals and the Limits of Precision in Molecular Timescales. Curr Biol. 25, 2939-2950.
10. Sebé-Pedrós A., Degnan B.M., and Ruiz-Trillo I. (2017). The origin of Metazoa: a unicellular perspective. Nature Reviews Genetics. 18, 498-512.
11. Queller D.C. (2000). Relatedness and the fraternal major transitions. Philos Trans R Soc Lond B Biol Sci. 355, 1647-1655.
12. Kraus Y., Chevalier S., and Houliston E. (2020). Cell shape changes during larval body plan development in Clytia hemisphaerica. Dev Biol. 468, 59-79.
13. Leys S.P., Cheung E., and Boury-Esnault N. (2006). Embryogenesis in the glass sponge Oopsacas minuta: Formation of syncytia by fusion of blastomeres. Integr Comp Biol. 46, 104-117.
14. Ryan J.F., Pang K., Schnitzler C.E., Nguyen A.D., Moreland R.T., Simmons D.K., Koch B.J., Francis W.R., Havlak P., NISC Comparative Sequencing Program et al. (2013). The genome of the ctenophore Mnemiopsis leidyi and its implications for cell type evolution. Science. 342, 1242592.
15. Eitel M., Guidi L., Hadrys H., Balsamo M., and Schierwater B. (2011). New insights into placozoan sexual reproduction and development. PLoS One. 6, e19639.
16. Spradling A.C. (2024). The Ancient Origin and Function of Germline Cysts. Results Probl Cell Differ. 71, 3-21.
17. Extavour C.G., and Akam M. (2003). Mechanisms of germ cell specification across the metazoans: epigenesis and preformation. Development. 130, 5869-5884.
18. Mikhailov K.V., Konstantinova A.V., Nikitin M.A., Troshin P.V., Rusin L.Y., Lyubetsky V.A., Panchin Y.V., Mylnikov A.P., Moroz L.L., Kumar S. et al. (2009). The origin of Metazoa: a transition from temporal to spatial cell differentiation. Bioessays. 31, 758-768.
19. Woodland H.R. (2016). The Birth of Animal Development: Multicellularity and the Germline. Curr Top Dev Biol. 117, 609-630.
20. Brunet T. (2023). Cell contractility in early animal evolution. Curr Biol. 33, R966-R985.
21. Balasubramanian M.K., Bi E., and Glotzer M. (2004). Comparative analysis of cytokinesis in budding yeast, fission yeast and animal cells. Curr Biol. 14, R806-18.
22. Hime G., and Saint R. (1992). Zygotic expression of the pebble locus is required for cytokinesis during the postblastoderm mitoses of Drosophila. Development. 114, 165-171.

23. Tatsumoto T., Xie X., Blumenthal R., Okamoto I., and Miki T. (1999). Human ECT2 is an exchange factor for Rho GTPases, phosphorylated in G2/M phases, and involved in cytokinesis. J Cell Biol. 147, 921-928.
24. Dechant R., and Glotzer M. (2003). Centrosome separation and central spindle assembly act in redundant pathways that regulate microtubule density and trigger cleavage furrow formation. Dev Cell. 4, 333-344.
25. Jantsch-Plunger V., Gönczy P., Romano A., Schnabel H., Hamill D., Schnabel R., Hyman A.A., and Glotzer M. (2000). CYK-4: A Rho family gtpase activating protein (GAP) required for central spindle formation and cytokinesis. J Cell Biol. 149, 1391-1404.
26. Mishima M., Kaitna S., and Glotzer M. (2002). Central spindle assembly and cytokinesis require a kinesin-like protein/RhoGAP complex with microtubule bundling activity. Dev Cell. 2, 41-54.
27. Niiya F., Xie X., Lee K.S., Inoue H., and Miki T. (2005). Inhibition of cyclin-dependent kinase 1 induces cytokinesis without chromosome segregation in an ECT2 and MgcRacGAP-dependent manner. J Biol Chem. 280, 36502-36509.
28. Yüce O., Piekny A.J., and Glotzer M. (2005). An ECT2-centralspindlin complex regulates the localization and function of RhoA. J Cell Biol. 170, 571-582.
29. Zhao W.-M., and Fang G. (2005). MgcRacGAP controls the assembly of the contractile ring and the initiation of cytokinesis. Proc Natl Acad Sci U S A. 102, 13158-13163.
30. Werner M., Munro E., and Glotzer M. (2007). Astral signals spatially bias cortical myosin recruitment to break symmetry and promote cytokinesis. Curr Biol. 17, 1286-1297.
31. Agromayor M., and Martin-Serrano J. (2013). Knowing when to cut and run: mechanisms that control cytokinetic abscission. Trends Cell Biol.
32. Lafaurie-Janvore J., Maiuri P., Wang I., Pinot M., Manneville J.-B., Betz T., Balland M., and Piel M. (2013). ESCRT-III assembly and cytokinetic abscission are induced by tension release in the intercellular bridge. Science. 339, 1625-1629.
33. Carlton J.G., Caballe A., Agromayor M., Kloc M., and Martin-Serrano J. (2012). ESCRT-III governs the Aurora B-mediated abscission checkpoint through CHMP4C. Science. 336, 220-225.
34. Guizetti J., Schermelleh L., Mäntler J., Maar S., Poser I., Leonhardt H., Müller-Reichert T., and Gerlich D.W. (2011). Cortical constriction during abscission involves helices of ESCRT-III-dependent filaments. Science. 331, 1616-1620.
35. Gai M., Camera P., Dema A., Bianchi F., Berto G., Scarpa E., Germena G., and Di Cunto F. (2011). Citron kinase controls abscission through RhoA and anillin. Mol Biol Cell. 22, 3768-3778.
36. Hernández-Plaza A., Szklarczyk D., Botas J., Cantalapiedra C.P., Giner-Lamia J., Mende D.R., Kirsch R., Rattei T., Letunic I., Jensen L.J. et al. (2023). eggNOG 6.0: enabling comparative genomics across 12 535 organisms. Nucleic Acids Res. 51, D389-D394.
37. Train C.-M., Pignatelli M., Altenhoff A., and Dessimoz C. (2019). iHam and pyHam: visualizing and processing hierarchical orthologous groups. Bioinformatics. 35, 2504-2506.
38. Altenhoff A.M., Warwick Vesztrocy A., Bernard C., Train C.M., Nicheperovich A., Prieto Baños S., Julca I., Moi D., Nevers Y., Majidian S. et al. (2024). OMA orthology in 2024: improved prokaryote coverage, ancestral and extant GO enrichment, a revamped synteny viewer and more in the OMA Ecosystem. Nucleic Acids Res. 52, D513-D521.
39. Wang J., Chitsaz F., Derbyshire M.K., Gonzales N.R., Gwadz M., Lu S., Marchler G.H., Song J.S., Thanki N., Yamashita R.A. et al. (2023). The conserved domain database in 2023. Nucleic Acids Res. 51, D384-D388.
40. Letunic I., Khedkar S., and Bork P. (2021). SMART: recent updates, new developments and status in 2020. Nucleic Acids Res. 49, D458-D460.
41. Paysan-Lafosse T., Blum M., Chuguransky S., Grego T., Pinto B.L., Salazar G.A., Bileschi M.L., Bork P., Bridge A., Colwell L. et al. (2023). InterPro in 2022. Nucleic Acids Res. 51, D418-D427.
42. Zhang D., and Glotzer M. (2015). The RhoGAP activity of CYK-4/MgcRacGAP functions non-canonically by promoting RhoA activation during cytokinesis. elife. 4, 204.

43. Pavicic-Kaltenbrunner V., Mishima M., and Glotzer M. (2007). Cooperative assembly of CYK-4/MgcRacGAP and ZEN-4/MKLP1 to form the centralspindlin complex. Mol Biol Cell. 18, 4992-5003.
44. White E.A., Raghuraman H., Perozo E., and Glotzer M. (2013). Binding of the CYK-4 subunit of the centralspindlin complex induces a large scale conformational change in the kinesin subunit. J Biol Chem. 288, 19785-19795.
45. Pan H., Guan R., Zhao R., Ou G., and Chen Z. (2021). Mechanistic insights into central spindle assembly mediated by the centralspindlin complex. Proc Natl Acad Sci U S A. 118, e2112039118.
46. Abramson J., Adler J., Dunger J., Evans R., Green T., Pritzel A., Ronneberger O., Willmore L., Ballard A.J., Bambrick J. et al. (2024). Accurate structure prediction of biomolecular interactions with AlphaFold 3. Nature. 630, 493-500.
47. Makyio H., Ohgi M., Takei T., Takahashi S., Takatsu H., Katoh Y., Hanai A., Ueda T., Kanaho Y., Xie Y. et al. (2012). Structural basis for Arf6-MKLP1 complex formation on the Flemming body responsible for cytokinesis. EMBO J. 1-14.
48. Saito S., Liu X.F., Kamijo K., Raziuddin R., Tatsumoto T., Okamoto I., Chen X., Lee C.C., Lorenzi M.V., Ohara N. et al. (2004). Deregulation and mislocalization of the cytokinesis regulator ECT2 activate the Rho signaling pathways leading to malignant transformation. J Biol Chem. 279, 7169-7179.
49. Gomez-Cavazos J.S., Lee K.-Y., Lara-González P., Li Y., Desai A., Shiau A.K., and Oegema K. (2020). A Non-canonical BRCT-Phosphopeptide Recognition Mechanism Underlies RhoA Activation in Cytokinesis. Curr Biol.
50. Zou Y., Shao Z., Peng J., Li F., Gong D., Wang C., Zuo X., Zhang Z., Wu J., Shi Y. et al. (2014). Crystal structure of triple-BRCT-domain of ECT2 and insights into the binding characteristics to CYK-4. FEBS Lett. 588, 2911-2920.
51. Wolfe B.A., Takaki T., Petronczki M., and Glotzer M. (2009). Polo-like kinase 1 directs assembly of the HsCyk-4 RhoGAP/Ect2 RhoGEF complex to initiate cleavage furrow formation. PLoS Biol. 7, e1000110.
52. Burkard M.E., Maciejowski J., Rodriguez-Bravo V., Repka M., Lowery D.M., Clauser K.R., Zhang C., Shokat K.M., Carr S.A., Yaffe M.B. et al. (2009). Plk1 self-organization and priming phosphorylation of HsCYK-4 at the spindle midzone regulate the onset of division in human cells. PLoS Biol. 7, e1000111.
53. Jumper J., Evans R., Pritzel A., Green T., Figurnov M., Ronneberger O., Tunyasuvunakool K., Bates R., Žídek A., Potapenko A. et al. (2021). Highly accurate protein structure prediction with AlphaFold. Nature. 596, 583-589.
54. Torruella G., Derelle R., Paps J., Lang B.F., Roger A.J., Shalchian-Tabrizi K., and Ruiz-Trillo I. (2012). Phylogenetic relationships within the Opisthokonta based on phylogenomic analyses of conserved single-copy protein domains. Mol Biol Evol. 29, 531-544.
55. Suga H., Chen Z., de Mendoza A., Sebé-Pedrós A., Brown M.W., Kramer E., Carr M., Kerner P., Vervoort M., Sánchez-Pons N. et al. (2013). The Capsaspora genome reveals a complex unicellular prehistory of animals. Nature Communications. 4, 246.
56. Brunet T., and King N. (2017). The origin of animal multicellularity and cell differentiation. Developmental Cell.
57. King N., Westbrook M.J., Young S.L., Kuo A., Abedin M., Chapman J., Fairclough S., Hellsten U., Isogai Y., Letunic I. et al. (2008). The genome of the choanoflagellate Monosiga brevicollis and the origin of metazoans. Nature. 451, 783-788.
58. Ruiz-Trillo I., Roger A.J., Burger G., Gray M.W., and Lang B.F. (2008). A phylogenomic investigation into the origin of metazoa. Mol Biol Evol. 25, 664-672.
59. Fairclough S.R., Dayel M.J., and King N. (2010). Multicellular development in a choanoflagellate. Curr Biol. 20, R875-6.
60. Dayel M.J., Alegado R.A., Fairclough S.R., Levin T.C., Nichols S.A., McDonald K., and King N. (2011). Cell differentiation and morphogenesis in the colony-forming choanoflagellate Salpingoeca rosetta. Dev Biol. 357, 73-82.

61. Toret C., Picco A., Boiero-Sanders M., Michelot A., and Kaksonen M. (2022). The cellular slime mold Fonticula alba forms a dynamic, multicellular collective while feeding on bacteria. Curr Biol. 32, 1961-1973.e4.
62. Sebé-Pedrós A., Irimia M., Del Campo J., Parra-Acero H., Russ C., Nusbaum C., Blencowe B.J., and Ruiz-Trillo I. (2013). Regulated aggregative multicellularity in a close unicellular relative of metazoa. Elife. 2, e01287.
63. Tolliday N., VerPlank L., and Li R. (2002). Rho1 directs formin-mediated actin ring assembly during budding yeast cytokinesis. Curr Biol. 12, 1864-1870.
64. Bi E., Maddox P., Lew D.J., Salmon E.D., McMillan J.N., Yeh E., and Pringle J.R. (1998). Involvement of an actomyosin contractile ring in Saccharomyces cerevisiae cytokinesis. J Cell Biol. 142, 1301-1312.
65. Daga R.R., and Chang F. (2005). Dynamic positioning of the fission yeast cell division plane. Proc Natl Acad Sci U S A. 102, 8228-8232.
66. Karpov S.A., and Leadbeater B.S.C. (1997). Cell and nuclear division in a freshwater choanoflagellate, Monosiga ovata Kent. European Journal of Protistology. 33, 323-334.
67. Nislow C., Lombillo V.A., Kuriyama R., and McIntosh J.R. (1992). A plus-end-directed motor enzyme that moves antiparallel microtubules in vitro localizes to the interzone of mitotic spindles. Nature. 359, 543-547.
68. Sellitto C., and Kuriyama R. (1988). Distribution of a matrix component of the midbody during the cell cycle in Chinese hamster ovary cells. J Cell Biol. 106, 431-439.
69. Hutterer A., Glotzer M., and Mishima M. (2009). Clustering of centralspindlin is essential for its accumulation to the central spindle and the midbody. Curr Biol. 19, 2043-2049.
70. Good M.C., Vahey M.D., Skandarajah A., Fletcher D.A., and Heald R. (2013). Cytoplasmic volume modulates spindle size during embryogenesis. Science. 342, 856-860.
71. Hazel J., Krutkramelis K., Mooney P., Tomschik M., Gerow K., Oakey J., and Gatlin J.C. (2013). Changes in cytoplasmic volume are sufficient to drive spindle scaling. Science. 342, 853-856.
72. Lekomtsev S., Su K.-C., Pye V.E., Blight K., Sundaramoorthy S., Takaki T., Collinson L.M., Cherepanov P., Divecha N., and Petronczki M. (2012). Centralspindlin links the mitotic spindle to the plasma membrane during cytokinesis. Nature. 492, 276-279.
73. Robinson D.N., and Cooley L. (1996). Stable intercellular bridges in development: the cytoskeleton lining the tunnel. Trends Cell Biol. 6, 474-479.
74. Ong S., and Tan C. (2010). Germline cyst formation and incomplete cytokinesis during Drosophila melanogaster oogenesis. Dev Biol. 337, 84-98.
75. Gerhold A.R., Labbé J.C., and Singh R. (2022). Uncoupling cell division and cytokinesis during germline development in metazoans. Front Cell Dev Biol. 10, 1001689.
76. Chaigne A., Labouesse C., White I.J., Agnew M., Hannezo E., Chalut K.J., and Paluch E.K. (2020). Abscission Couples Cell Division to Embryonic Stem Cell Fate. Dev Cell. 55, 195-208.e5.
77. Adar-Levor S., Nachmias D., Gal-Oz S.T., Jahn Y.M., Peyrieras N., Zaritsky A., Birnbaum R.Y., and Elia N. (2021). Cytokinetic abscission is part of the midblastula transition in early zebrafish embryogenesis. Proc Natl Acad Sci U S A. 118, e2021210118.
78. Cartwright J., and Arnold J.M. (1981). Intercellular bridges in the embryo of the Atlantic squid, Loligo pealei. II: Formation of the bridge. Cell Motil. 1, 455-468.
79. Fawcett D.W., Ito S., and Slautterback D. (1959). The occurrence of intercellular bridges in groups of cells exhibiting synchronous differentiation. J Biophys Biochem Cytol. 5, 453-460.
80. McLean P.F., and Cooley L. (2013). Protein equilibration through somatic ring canals in Drosophila. Science. 340, 1445-1447.
81. Mahajan-Miklos S., and Cooley L. (1994). Intercellular cytoplasm transport during Drosophila oogenesis. Dev Biol. 165, 336-351.
82. Lu W., Lakonishok M., Serpinskaya A.S., and Gelfand V.I. (2022). A novel mechanism of bulk cytoplasmic transport by cortical dynein in Drosophila ovary. Elife. 11, e75538.

83. Lee K.Y., Green R.A., Gutierrez E., Gomez-Cavazos J.S., Kolotuev I., Wang S., Desai A., Groisman A., and Oegema K. (2018). CYK-4 functions independently of its centralspindlin partner ZEN-4 to cellularize oocytes in germline syncytia. Elife. 7, e36919.
84. Wong H.N., Chen T., Wang P.J., and Holzman L.B. (2024). ARF6, a component of intercellular bridges, is essential for spermatogenesis in mice. Dev Biol. 508, 46-63.
85. Knoblich J.A., Jan L.Y., and Jan Y.N. (1995). Asymmetric segregation of Numb and Prospero during cell division. Nature. 377, 624-627.
86. Kemphues K. (2000). PARsing embryonic polarity. Cell. 101, 345-348.
87. Zenker J., White M.D., Templin R.M., Parton R.G., Thorn-Seshold O., Bissiere S., and Plachta N. (2017). A microtubule-organizing center directing intracellular transport in the early mouse embryo. Science. 357, 925-928.
88. Gazave E., Lapébie P., Richards G.S., Brunet F., Ereskovsky A.V., Degnan B.M., Borchiellini C., Vervoort M., and Renard E. (2009). Origin and evolution of the Notch signalling pathway: an overview from eukaryotic genomes. BMC Evol Biol. 9, 249.
89. Derivery E., Seum C., Daeden A., Loubéry S., Holtzer L., Jülicher F., and González-Gaitán M. (2015). Polarized endosome dynamics by spindle asymmetry during asymmetric cell division. Nature. 528, 280-285.
90. Guillot C., and Lecuit T. (2013). Adhesion disengagement uncouples intrinsic and extrinsic forces to drive cytokinesis in epithelial tissues. Dev Cell. 24, 227-241.
91. Jesuthasan S. (1998). Furrow-associated microtubule arrays are required for the cohesion of zebrafish blastomeres following cytokinesis. J Cell Sci. 111, 3695-3703.
92. Reinsch S., and Karsenti E. (1994). Orientation of spindle axis and distribution of plasma membrane proteins during cell division in polarized MDCKII cells. J Cell Biol. 126, 1509-1526.
93. Drechsel D.N., Hyman A.A., Hall A., and Glotzer M. (1997). A requirement for Rho and Cdc42 during cytokinesis in Xenopus embryos. Curr Biol. 7, 12-23.
94. Sulston J.E., and Horvitz H.R. (1977). Post-embryonic cell lineages of the nematode, Caenorhabditis elegans. Dev Biol. 56, 110-156.
95. Sulston J.E., Schierenberg E., White J.G., and Thomson J.N. (1983). The embryonic cell lineage of the nematode Caenorhabditis elegans. Dev Biol. 100, 64-119.
96. Umen J.G. (2014). Green algae and the origins of multicellularity in the plant kingdom. Cold Spring Harb Perspect Biol. 6, a016170.
97. Green K.J., Viamontes G.I., and Kirk D.L. (1981). Mechanism of formation, ultrastructure, and function of the cytoplasmic bridge system during morphogenesis in Volvox. J Cell Biol. 91, 756-769.
98. UniProt Consortium. (2023). UniProt: the Universal Protein Knowledgebase in 2023. Nucleic Acids Res. 51, D523-D531.
99. Sayers E.W., Bolton E.E., Brister J.R., Canese K., Chan J., Comeau D.C., Connor R., Funk K., Kelly C., Kim S. et al. (2022). Database resources of the national center for biotechnology information. Nucleic Acids Res. 50, D20-D26.
100. Varadi M., Bertoni D., Magana P., Paramval U., Pidruchna I., Radhakrishnan M., Tsenkov M., Nair S., Mirdita M., Yeo J. et al. (2024). AlphaFold Protein Structure Database in 2024: providing structure coverage for over 214 million protein sequences. Nucleic Acids Res. 52, D368-D375.
101. Sievers F., and Higgins D.G. (2018). Clustal Omega for making accurate alignments of many protein sequences. Protein Sci. 27, 135-145.
102. McDonnell A.V., Jiang T., Keating A.E., and Berger B. (2006). Paircoil2: improved prediction of coiled coils from sequence. Bioinformatics. 22, 356-358.

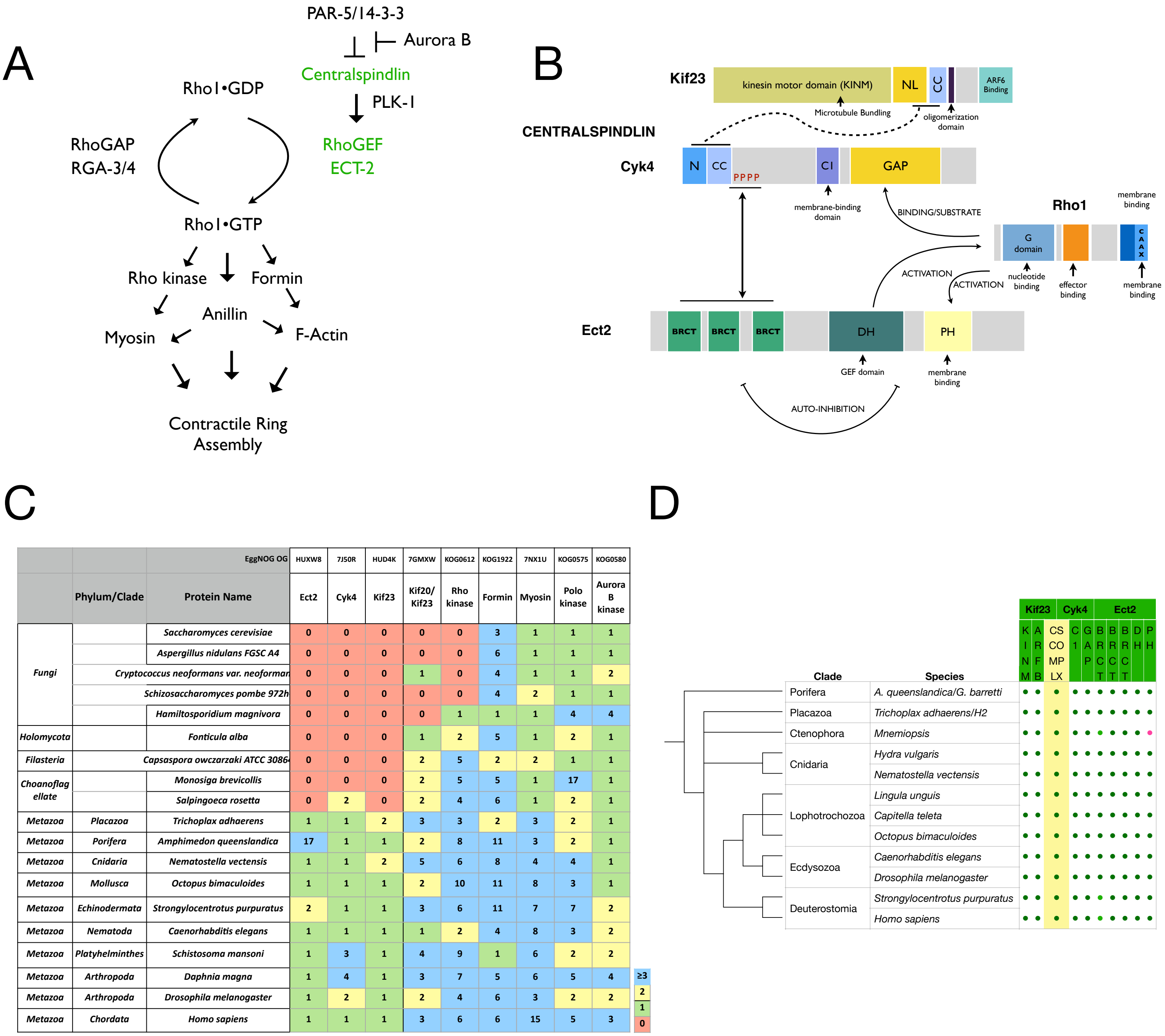
A
PAR-5/14-3-3
Aurora B
Centralspindlin
PLK-1
RhoGEF
ECT-2
Rho1•GDP
RhoGAP
RGA-3/4
Rho1•GTP
Rho kinase
Formin
Anillin
Myosin
F-Actin
Contractile Ring
Assembly
B
Kif23
kinesin motor domain (KINM)
NL
CC
ARF6
Binding
Microtubule Bundling
oligomerization
domain
CENTRALSPINDLIN
Cyk4
N
CC
PPPP
CI
GAP
membrane-binding
domain
BINDING/SUBSTRATE
Rho1
membrane
binding
G
domain
C
A
A
X
nucleotide
binding
effector
binding
membrane
binding
ACTIVATION
ACTIVATION
Ect2
BRCT
BRCT
BRCT
DH
PH
GEF domain
membrane
binding
AUTO-INHIBITION
C
≥3
2
1
0
D

		EggNOG OG	HUXW8	7J50R	HUD4K	7GMXW	KOG0612	KOG1922	7NX1U	KOG0575	KOG0580
	Phylum/Clade	Protein Name	Ect2	Cyk4	Kif23	Kif20/ Kif23	Rho kinase	Formin	Myosin	Polo kinase	Aurora B kinase
Fungi		*Saccharomyces cerevisiae*	0	0	0	0	0	3	1	1	1
		Aspergillus nidulans FGSC A4	0	0	0	0	0	6	1	1	1
		Cryptococcus neoformans var. neoforman	0	0	0	1	0	4	1	1	2
		Schizosaccharomyces pombe 972h	0	0	0	0	0	4	2	1	1
		Hamiltosporidium magnivora	0	0	0	0	1	1	1	4	4
Holomycota		*Fonticula alba*	0	0	0	1	2	5	1	2	1
Filasteria		*Capsaspora owczarzaki ATCC 3086*	0	0	0	2	5	2	2	1	1
Choanoflagellate		*Monosiga brevicollis*	0	0	0	2	5	5	1	17	1
		Salpingoeca rosetta	0	2	0	2	4	6	1	2	1
Metazoa	*Placazoa*	*Trichoplax adhaerens*	1	1	2	3	3	2	3	2	1
Metazoa	*Porifera*	*Amphimedon queenslandica*	17	1	1	2	8	11	3	2	1
Metazoa	*Cnidaria*	*Nematostella vectensis*	1	1	2	5	6	8	4	4	1
Metazoa	*Mollusca*	*Octopus bimaculoides*	1	1	1	2	10	11	8	3	1
Metazoa	*Echinodermata*	*Strongylocentrotus purpuratus*	2	1	1	3	6	11	7	7	2
Metazoa	*Nematoda*	*Caenorhabditis elegans*	1	1	1	1	2	4	8	3	2
Metazoa	*Platyhelminthes*	*Schistosoma mansoni*	1	3	1	4	9	1	6	2	2
Metazoa	*Arthropoda*	*Daphnia magna*	1	4	1	3	7	5	6	5	4
Metazoa	*Arthropoda*	*Drosophila melanogaster*	1	2	1	2	4	6	3	2	2
Metazoa	*Chordata*	*Homo sapiens*	1	1	1	3	6	6	15	5	3

		Kif23			Cyk4		Ect2				
Clade	Species	KINM	ARFB	CSCOMPLX	C1	GAP	BRCT	BRCT	BRCT	DH	PH
Porifera	*A. queenslandica/G. barretti*	●	●	●	●	●	●	●	●	●	●
Placazoa	*Trichoplax adhaerens/H2*	●	●	●	●	●	●	●	●	●	●
Ctenophora	*Mnemiopsis*	●	●	●	●	●	●	●	●	●	●
Cnidaria	*Hydra vulgaris*	●	●	●	●	●	●	●	●	●	●
	Nematostella vectensis	●	●	●	●	●	●	●	●	●	●
Lophotrochozoa	*Lingula unguis*	●	●	●	●	●	●	●	●	●	●
	Capitella teleta	●	●	●	●	●	●	●	●	●	●
	Octopus bimaculoides	●	●	●	●	●	●	●	●	●	●
Ecdysozoa	*Caenorhabditis elegans*	●	●	●	●	●	●	●	●	●	●
	Drosophila melanogaster	●	●	●	●	●	●	●	●	●	●
Deuterostomia	*Strongylocentrotus purpuratus*	●	●	●	●	●	●	●	●	●	●
	Homo sapiens	●	●	●	●	●	●	●	●	●	●

Figure 1 Centralspindlin and Ect2 regulate Rho1 activation and are structurally conserved in all clades of Metazoa

A. Schematic depicting the Rho1-dependent pathway for contractile ring assembly in Metazoa. B. Detailed map of the known interactions between Centralspindlin, Ect2, and Rho1 (see text for details). C. The number of orthologs of each species that belong to each of the indicated (top) EggNOG orthologous groups. D. Presence (green dot), or absence (pink dot) of each structural domain in the Metazoan representatives of Kif23, Cyk4, and Ect2. A lighter green dot indicates less confidence in the structural prediction. The integrity of each domain was assessed by a combination of SMART, Interpro, CDD-NCBI and the Alphafold predictions. Complex formation was assessed with Alphafold3. The apparent absence of Ect2 PH domain in Ctenophora may reflect the preliminary state of the Mnemiopsis genome sequence (see methods).

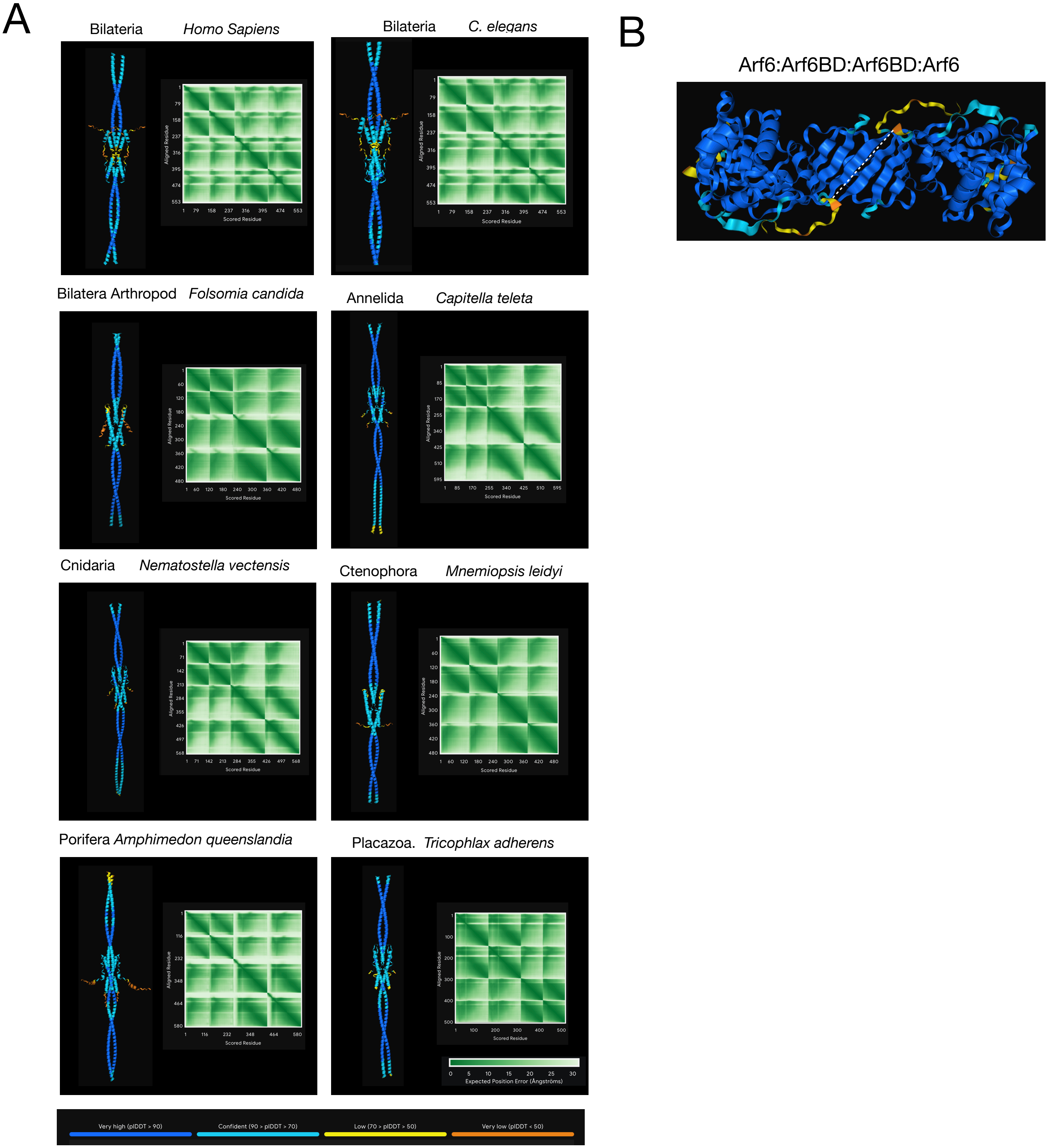
A
Bilateria Homo Sapiens
Bilateria C. elegans
Bilatera Arthropod Folsomia candida
Annelida Capitella teleta
Cnidaria Nematostella vectensis
Ctenophora Mnemiopsis leidyi
Porifera Amphimedon queenslandia
Placazoa. Tricophlax adherens
Aligned Residue
Scored Residue
Expected Position Error (Ångströms)
Very high (pLDDT > 90)
Confident (90 > pLDDT > 70)
Low (70 > pLDDT > 50)
Very low (pLDDT < 50)
B
Arf6:Arf6BD:Arf6BD:Arf6

Figure 2 The interaction between Kif23 and Cyk4 is conserved among Metazoa.

A. The region of Cyk4 from the N-terminus to the end of the coiled coil and the region of Kif23 from the end of the motor domain to the end of the coiled coil were used to generate Alphafold3 predictions. Predictions were refined by trimming unstructured regions. Inter-subunit interactions are indicated by the turquoise and blue interacting regions and the low predicted aligned errors (dark green) in the top right/bottom left regions of the 2D plots.

B. The H.s. Arf6 binding domain and Hs Arf6 were used to generate Alphafold3 predicted structures.

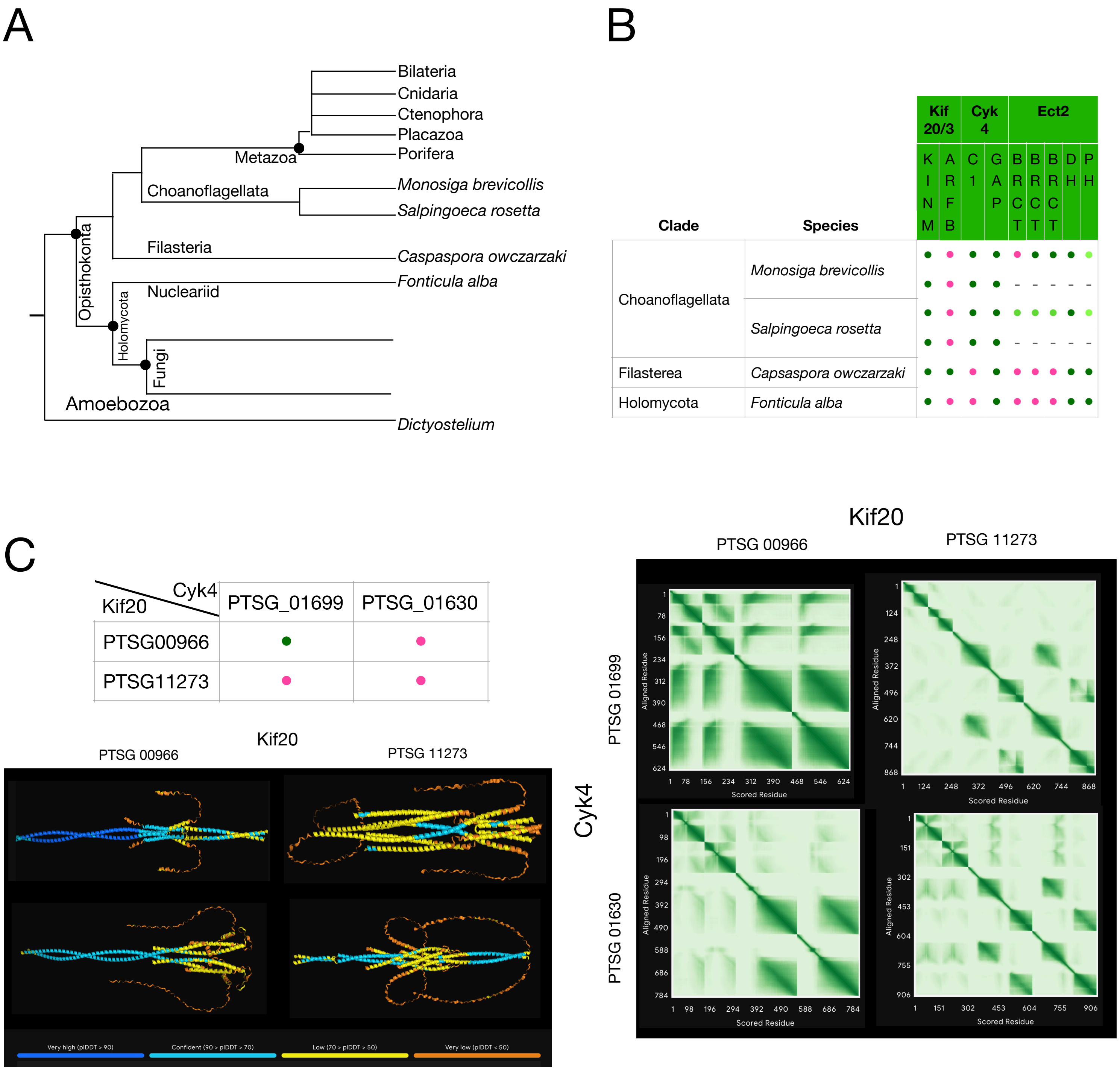
A
Bilateria
Cnidaria
Ctenophora
Placazoa
Porifera
Metazoa
Choanoflagellata
Monosiga brevicollis
Salpingoeca rosetta
Opisthokonta
Filasteria
Caspaspora owczarzaki
Nucleariid
Fonticula alba
Holomycota
Fungi
Amoebozoa
Dictyostelium
B
C
Kif20
PTSG 00966
PTSG 11273
Cyk4
PTSG 01699
PTSG 01630
Very high (pIDDT > 90)
Confident (90 > pIDDT > 70)
Low (70 > pIDDT > 50)
Very low (pIDDT < 50)
Aligned Residue
Scored Residue

B

Clade	Species	Kif 20/3		Cyk 4		Ect2				
		KINM	ARFB	C1	GAP	BRCT	BRCT	BRCT	DH	PH
Choanoflagellata	*Monosiga brevicollis*	🟢	🔴	🟢	🟢	🔴	🟢	🟢	🟢	🟩
		🟢	🔴	🟢	🟢	-	-	-	-	-
	Salpingoeca rosetta	🟢	🔴	🟢	🟢	🟩	🟩	🟩	🟢	🟩
		🟢	🔴	🟢	🟢	-	-	-	-	-
Filasterea	*Capsaspora owczarzaki*	🟢	🟢	🔴	🟢	🔴	🔴	🔴	🟢	🟢
Holomycota	*Fonticula alba*	🟢	🔴	🔴	🟢	🔴	🔴	🔴	🟢	🟢

C

Kif20 \ Cyk4	PTSG_01699	PTSG_01630
PTSG00966	🟢	🔴
PTSG11273	🔴	🔴

Figure 3. The taxonomic neighbors of Metazoa have centralspindlin-like properties.

A. Phylogenetic tree of Metazoa and taxonomic neighbors. B. Presence (green dot; light green indicates more flexibility in the structural predictions) or absence (pink) of Kif20/23, Cyk4, and Ect2 related proteins in the indicated species. Dashes indicate absence of a paralog. C. Structural predictions of the 4 possible combinations of the 2 paralogs of Kif20 and Cyk4 generated using Alphafold3. Note that only PTSG00966/PTSG 01699 are confidently predicted to form a complex.

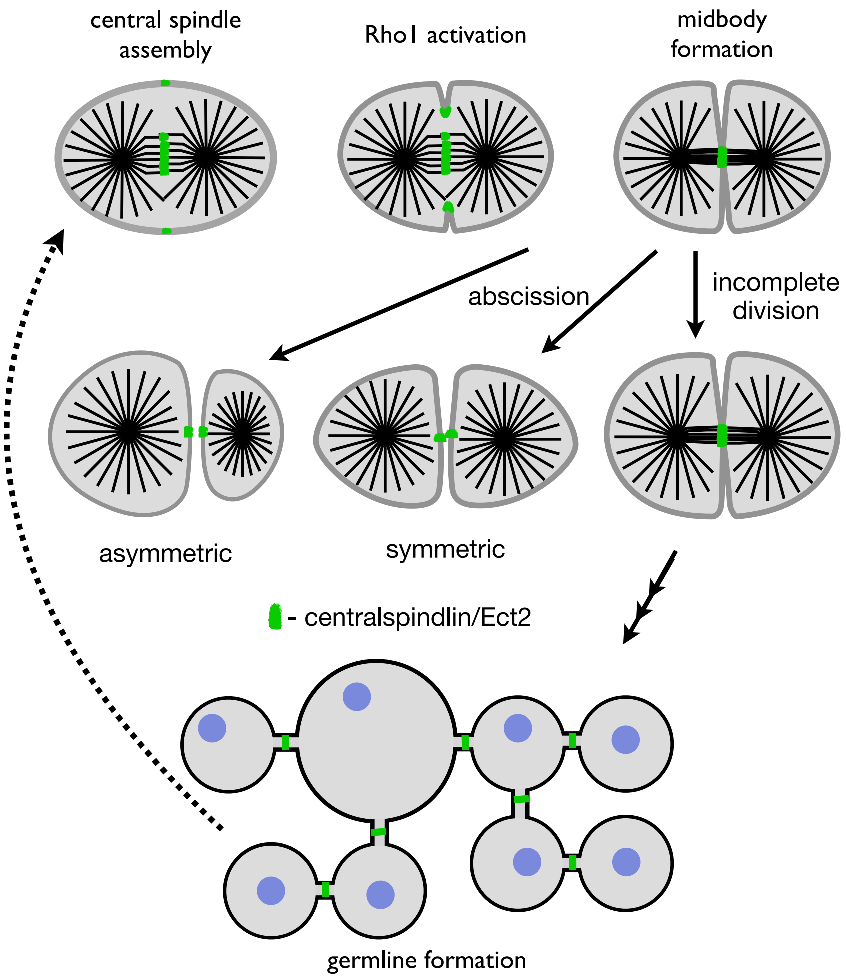
central spindle assembly
Rho1 activation
midbody formation
abscission
incomplete division
asymmetric
symmetric
🟩 - centralspindlin/Ect2
germline formation

Figure 4. Model depicting a subset of the functions of centralspindlin/Ect2 that are ubiquitous in Metazoa and likely contributed to Metazoa and multicellularity. Centralspindlin/Ect2 promote central spindle assembly, spindle-directed Rho1 activation and midbody and intercellular bridge formation. These functions enable symmetric and asymmetric division of variably sized cells, under the control of the position of the spindle, as well as incomplete division, which is implicated involved in gamete formation (see text for details).

A

Kif23 Identity matrix

	1	2	3	4	5	6	7	8	9	10	11	12	13	14	15	16	17	18
1 Fonticula		22.38	23.64	22.06	24.08	23.73	24.50	22.29	24.68	23.77	23.99	25.12	23.68	24.04	24.15	24.20	21.56	29.76
2 M_brev (24755)	22.38		35.98	25.75	28.45	25.00	27.40	23.48	26.41	27.62	27.59	29.13	27.86	27.84	25.15	25.75	22.83	35.23
3 S_rosetta (11273)	23.64	35.98		26.36	26.99	27.35	27.95	26.22	28.53	25.27	27.65	29.40	26.19	27.33	25.17	26.08	25.19	34.69
4 Drosophila	22.06	25.75	26.36		39.24	38.17	43.64	41.85	38.46	41.11	40.02	39.45	41.85	34.87	35.32	32.25	26.95	37.31
5 Amphimedon	24.08	28.45	26.99	39.24		37.52	43.33	41.32	41.64	42.65	40.05	42.72	44.70	32.34	37.39	31.36	27.49	40.91
6 Octopus	23.73	25.00	27.35	38.17	37.52		45.41	41.64	37.78	38.92	36.14	38.27	39.88	33.69	33.63	29.46	25.48	37.17
7 Lingula	24.50	27.40	27.95	43.64	43.33	45.41		53.51	41.51	44.77	42.19	46.29	50.00	34.20	39.63	32.74	28.59	39.55
8 Capitella	22.29	23.48	26.22	41.85	41.32	41.64	53.51		38.63	41.79	41.08	44.25	47.03	35.41	37.23	31.70	25.81	39.70
9 Trichoplax	24.68	26.41	28.53	38.46	41.64	37.78	41.51	38.63		42.29	41.97	49.77	45.59	34.38	37.18	32.42	31.22	41.51
10 Homo	23.77	27.62	25.27	41.11	42.65	38.92	44.77	41.79	42.29		42.89	47.18	49.70	34.97	37.23	30.98	26.72	38.75
11 Hydra	23.99	27.59	27.65	40.02	40.05	36.14	42.19	41.08	41.97	42.89		48.95	45.76	32.98	39.95	32.01	27.56	39.33
12 Nematostella	25.12	29.13	29.40	39.45	42.72	38.27	46.29	44.25	49.77	47.18	48.95		50.24	33.03	39.69	30.98	28.61	36.90
13 Strongylocentrotus	23.68	27.86	26.19	41.85	44.70	39.88	50.00	47.03	45.59	49.70	45.76	50.24		37.81	41.97	31.53	28.02	37.69
14 Caenorhabditis	24.04	27.84	27.33	34.87	32.34	33.69	34.20	35.41	34.38	34.97	32.98	33.03	37.81		31.84	30.80	26.06	37.89
15 Mnemiopsis	24.15	25.15	25.17	35.32	37.39	33.63	39.63	37.23	37.18	37.23	39.95	39.69	41.97	31.84		31.59	28.10	38.13
16 Capsaspora	24.20	25.75	26.08	32.25	31.36	29.46	32.74	31.70	32.42	30.98	32.01	30.98	31.53	30.80	31.59		30.23	40.43
17 S. rosetta (00966)	21.56	22.83	25.19	26.95	27.49	25.48	28.59	25.81	31.22	26.72	27.56	28.61	28.02	26.06	28.10	30.23		40.89
18 M_brev (13496) (motor domain only)	29.76	35.23	34.69	37.31	40.91	37.17	39.55	39.70	41.51	38.75	39.33	36.90	37.69	37.89	38.13	40.43	40.89	

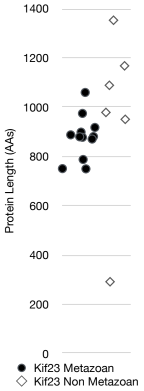

B

Cyk4 Identity matrix

	1	2	3	4	5	6	7	8	9	10	11	12	13	14	15	16	17	18
1 Monosiga A9V1W6		31.79	16.06	17.29	15.66	16.57	16.67	15.90	14.02	18.27	18.62	17.02	16.39	18.88	19.83	18.11	16.80	17.41
2 Salpingoeca XP_004997677.1	31.79		19.44	19.03	16.49	17.62	17.94	17.01	20.16	20.33	21.48	19.76	21.80	21.72	22.62	20.99	20.48	21.83
3 Monosiga XP_001749975.1	16.06	19.44		29.80	15.31	17.70	20.14	19.00	17.78	18.78	21.47	19.83	20.61	20.26	22.39	21.68	20.93	23.02
4 Salpingoeca XP_004997610.1	17.29	19.03	29.80		14.29	17.20	20.44	19.67	21.31	19.28	23.64	22.18	21.74	23.00	22.29	21.56	21.54	24.80
5 Fonticula	15.66	16.49	15.31	14.29		19.08	18.36	15.43	17.69	17.47	20.00	19.33	21.46	19.17	20.40	20.30	19.96	17.71
6 Caenorhabditis	16.57	17.62	17.70	17.20	19.08		21.48	20.11	19.93	21.22	24.24	21.38	23.77	24.28	24.14	22.30	23.79	25.27
7 Amphimedon	16.67	17.94	20.14	20.44	18.36	21.48		28.89	29.11	27.29	29.15	29.15	28.16	30.78	33.45	32.25	32.81	32.51
8 Mnemiopsis	15.90	17.01	19.00	19.67	15.43	20.11	28.89		28.76	24.07	32.89	28.40	28.81	32.01	32.30	30.55	30.20	31.36
9 Folsomia	14.02	20.16	17.78	21.31	17.69	19.93	29.11	28.76		33.46	33.64	31.33	32.07	33.27	34.82	34.73	37.55	37.89
10 Drosophila	18.27	20.33	18.78	19.28	17.47	21.22	27.29	24.07	33.46		31.98	29.28	33.03	34.90	32.38	32.39	35.70	36.51
11 Trichoplax	18.62	21.48	21.47	23.64	20.00	24.24	29.15	32.89	33.64	31.98		37.16	37.68	40.79	43.18	42.37	40.89	44.89
12 Hydra	17.02	19.76	19.83	22.18	19.33	21.38	29.15	28.40	31.33	29.28	37.16		36.20	38.53	38.33	42.23	38.23	37.23
13 Octopus	16.39	21.80	20.61	21.74	21.46	23.77	28.16	28.81	32.07	33.03	37.68	36.20		37.35	33.98	39.69	42.91	43.71
14 Homo	18.88	21.72	20.26	23.00	19.17	24.28	30.78	32.01	33.27	34.90	40.79	38.53	37.35		45.69	44.43	41.77	44.01
15 Strongylocentrotus	19.83	22.62	22.39	22.29	20.40	24.14	33.45	32.30	34.82	32.38	43.18	38.33	33.98	45.69		47.32	44.81	48.64
16 Nematostella	18.11	20.99	21.68	21.56	20.30	22.30	32.25	30.55	34.73	32.39	42.37	42.23	39.69	44.43	47.32		45.84	47.32
17 Capitella	16.80	20.48	20.93	21.54	19.96	23.79	32.81	30.20	37.55	35.70	40.89	38.23	42.91	41.77	44.81	45.84		57.31
18 Lingula	17.41	21.83	23.02	24.80	17.71	25.27	32.51	31.36	37.89	36.51	44.89	37.23	43.71	44.01	48.64	47.32	57.31	

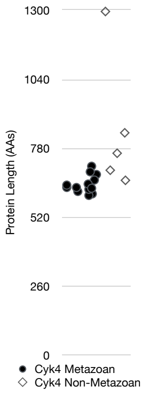

C

Ect2 Identity matrix

	1	2	3	4	5	6	7	8	9	10	11	12	13	14	15	16
1 Capsaspora		23.55	20.53	27.79	26.24	30.05	24.60	26.29	25.27	24.90	27.71	25.15	30.59	19.33	19.12	21.72
2 Mnemiopsis	23.55		19.24	21.15	22.04	22.12	21.68	22.60	23.01	23.26	23.88	23.64	21.38	15.11	17.00	16.13
3 Caenorhabditis	20.53	19.24		22.41	22.89	25.43	24.01	24.71	23.33	22.94	22.70	24.25	21.84	15.01	13.79	15.82
4 Geodia	27.79	21.15	22.41		32.46	33.95	34.41	37.86	36.99	34.83	35.98	39.31	40.20	15.12	17.96	18.24
5 Drosophila	26.24	22.04	22.89	32.46		34.16	39.16	39.09	40.77	35.80	35.29	36.71	34.30	15.18	15.59	18.15
6 Hydra	30.05	22.12	25.43	33.95	34.16		37.23	39.36	39.50	38.27	39.45	42.72	38.40	15.38	16.31	16.91
7 Octopus	24.60	21.68	24.01	34.41	39.16	37.23		43.88	44.19	38.31	41.66	40.53	37.78	15.01	15.26	15.40
8 Lingula	26.29	22.60	24.71	37.86	39.09	39.36	43.88		52.07	41.59	42.87	44.19	39.31	16.64	15.73	15.88
9 Capitella	25.27	23.01	23.33	36.99	40.77	39.50	44.19	52.07		43.63	42.01	44.07	40.73	14.72	15.59	15.60
10 Strongylocentrotus	24.90	23.26	22.94	34.83	35.80	38.27	38.31	41.59	43.63		42.79	42.95	39.97	15.63	17.91	16.28
11 Homo	27.71	23.88	22.70	35.98	35.29	39.45	41.66	42.87	42.01	42.79		44.97	41.93	16.08	19.40	16.41
12 Nematostella	25.15	23.64	24.25	39.31	36.71	42.72	40.53	44.19	44.07	42.95	44.97		45.04	17.18	18.37	18.34
13 Trichoplax	30.59	21.38	21.84	40.20	34.30	38.40	37.78	39.31	40.73	39.97	41.93	45.04		15.38	18.51	15.70
14 Fonticula	19.33	15.11	15.01	15.12	15.18	15.38	15.01	16.64	14.72	15.63	16.08	17.18	15.38		18.35	17.59
15 Salpingoeca	19.12	17.00	13.79	17.96	15.59	16.31	15.26	15.73	15.59	17.91	19.40	18.37	18.51	18.35		26.05
16 Monosiga	21.72	16.13	15.82	18.24	18.15	16.91	15.40	15.88	15.60	16.28	16.41	18.34	15.70	17.59	26.05	

≥
40
30
20
10

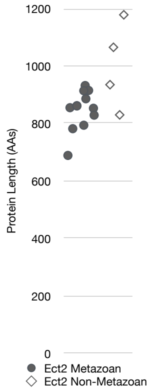

Supplemental figure 1 Sequence conservation of Kif23, Cyk4, and Ect2. A. Pairwise identity matrices and overall lengths of the proteins analyzed in detail in this study: (A) Kif20/23 (B) Cyk4, and (C) Ect2. Blue ≥ 10% identity, teal ≥ 30% identity; green ≥ 30% identity; yellow ≥ 40% identity. Protein lengths for orthologs of Kif23, Cyk4, and Ect2. Graphs compare the size in amino acids of Metazoan orthologs (•) and non-metazoan orthologs (◇).

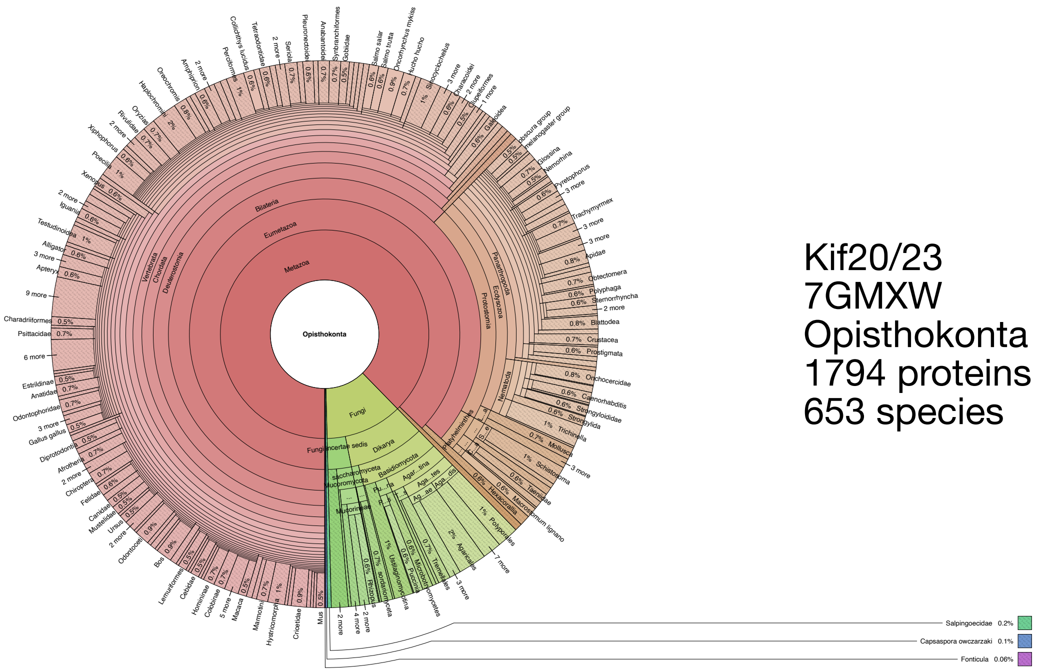

Kif20/23
7GMXW
Opisthokonta
1794 proteins
653 species

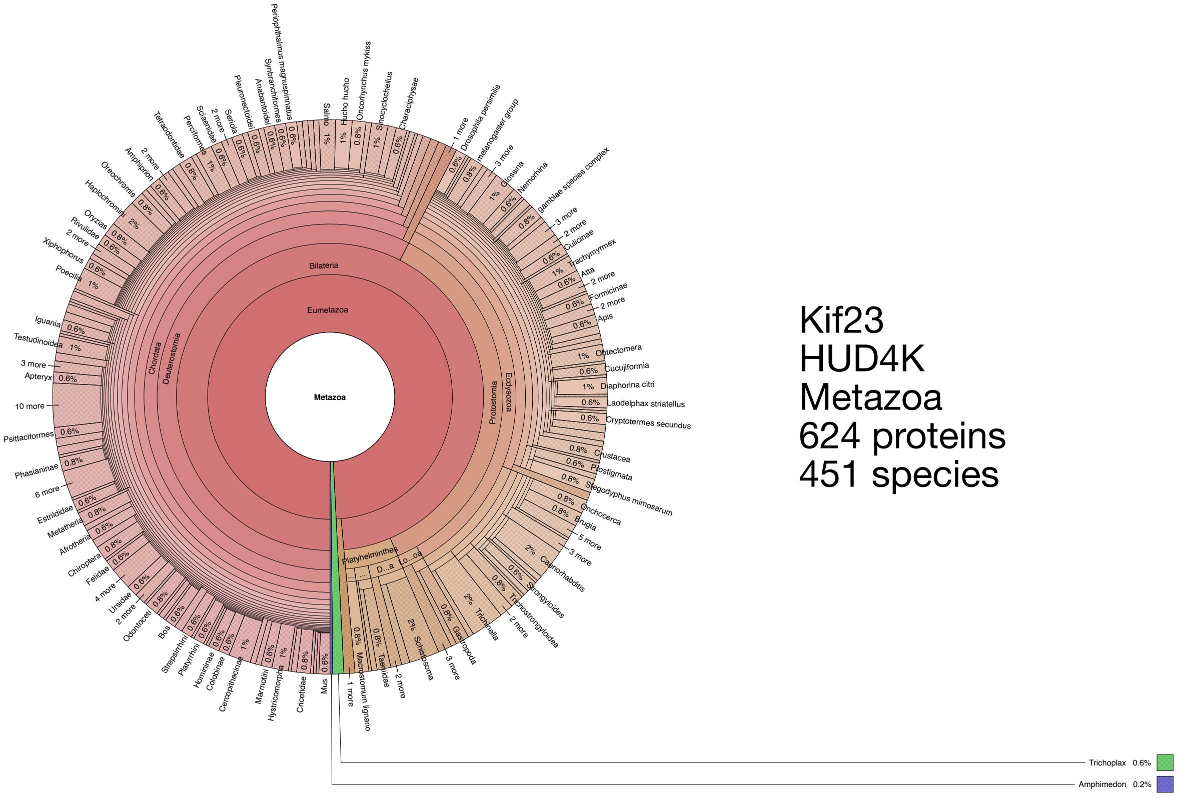

Kif23
HUD4K
Metazoa
624 proteins
451 species

Supplemental figure 2. Kif23 is a kinesin-6 family member found in metazoa; Kif20 is found in both metazoa and fungi.The taxonomic distribution of the Kif20/23 unsupervised orthologous group 7GMXW and the Kif23 child group HUD4K. Source EggNOGv6.

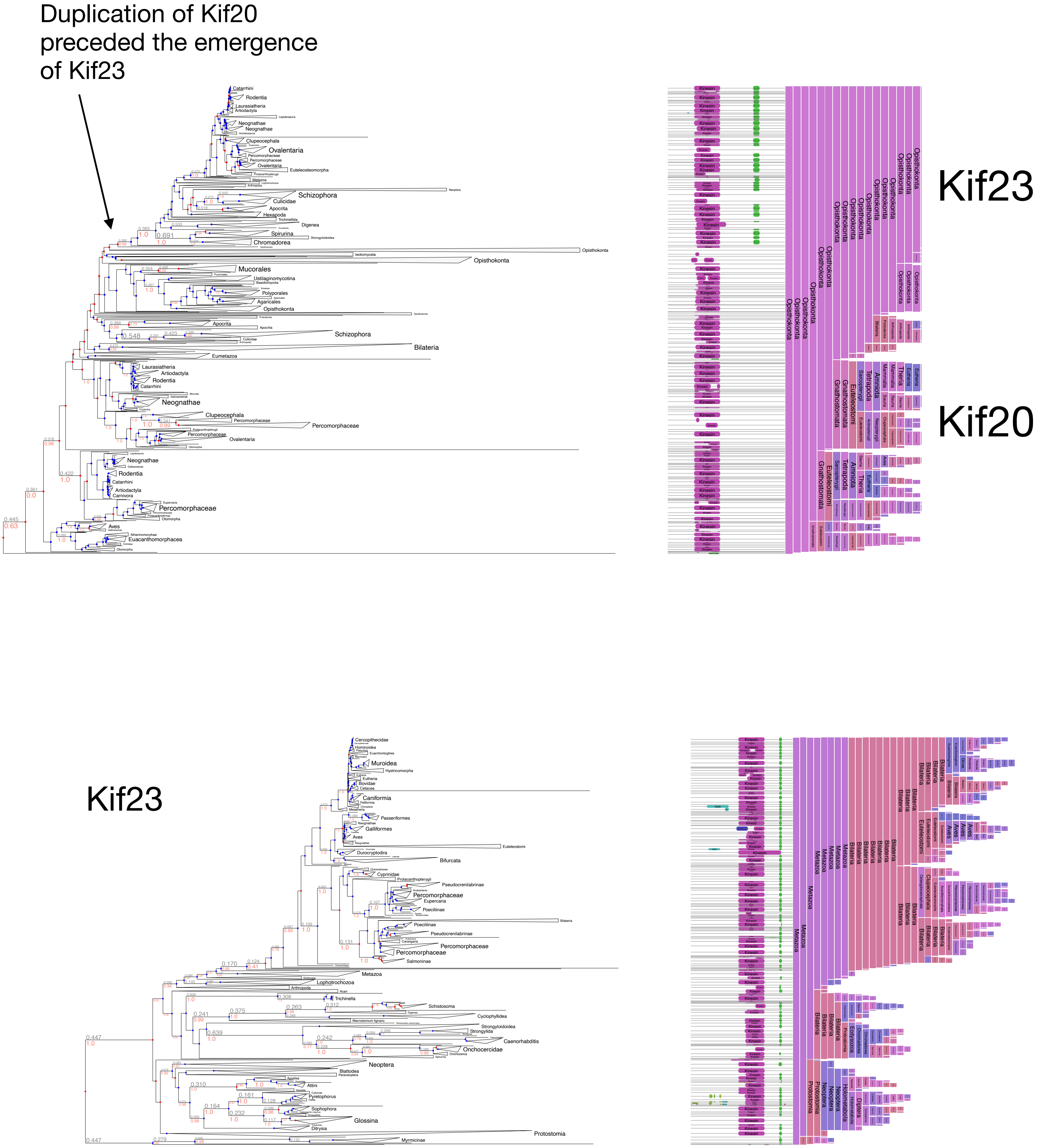

Duplication of Kif20 preceded the emergence of Kif23

Kif23
Kif20
Kif23
Catarrhini
Rodentia
Laurasiatheria
Artiodactyla
Neognathae
Clupeocephala
Ovalentaria
Percomorphaceae
Euteleosteomorpha
Schizophora
Culicidae
Apocrita
Hexapoda
Digenea
Spirurina
Chromadorea
Opisthokonta
Mucorales
Ustilaginomycotina
Polyporales
Agaricales
Apocrita
Schizophora
Bilateria
Eumetazoa
Neognathae
Clupeocephala
Percomorphaceae
Ovalentaria
Rodentia
Catarrhini
Artiodactyla
Carnivora
Aves
Euacanthomorphacea
Kinesin
Gnathostomata
Euteleostomi
Sarcopterygii
Tetrapoda
Amniota
Mammalia
Theria
Eutheria
Cercopithecidae
Hominoidea
Muroidea
Caniformia
Passeriformes
Galliformes
Euteleostomi
Bifurcata
Cypriniidae
Pseudocrenilabrinae
Percomorphaceae
Poeciliinae
Salmoninae
Metazoa
Lophotrochozoa
Arthropoda
Trichinella
Schistosoma
Cyclophyllidea
Strongyloidoidea
Caenorhabditis
Onchocercidae
Neoptera
Blattodea
Anopheles
Pyretophorus
Sophophora
Glossina
Ditrysia
Protostomia
Myrmicinae
Ecdysozoa
Holometabola
Diptera

Supplemental figure 3. Taxonomic tree of the Kif20/23 unsupervised orthologous group 7GMXW (top) and the Kif23 child group HUD4K, which resulted from a gene duplication (red dots; blue dots indicate speciation events). Note the Arf6 binding domain is unique to Kif23. The extra N-terminal domains of Kif23 (bottom) are prevalent in various Anopheles species, perhaps indicating an evolutionary response to Malaria. Bars on the right indicate the last common ancestor of the corresponding proteins. Source EggNOGv6.

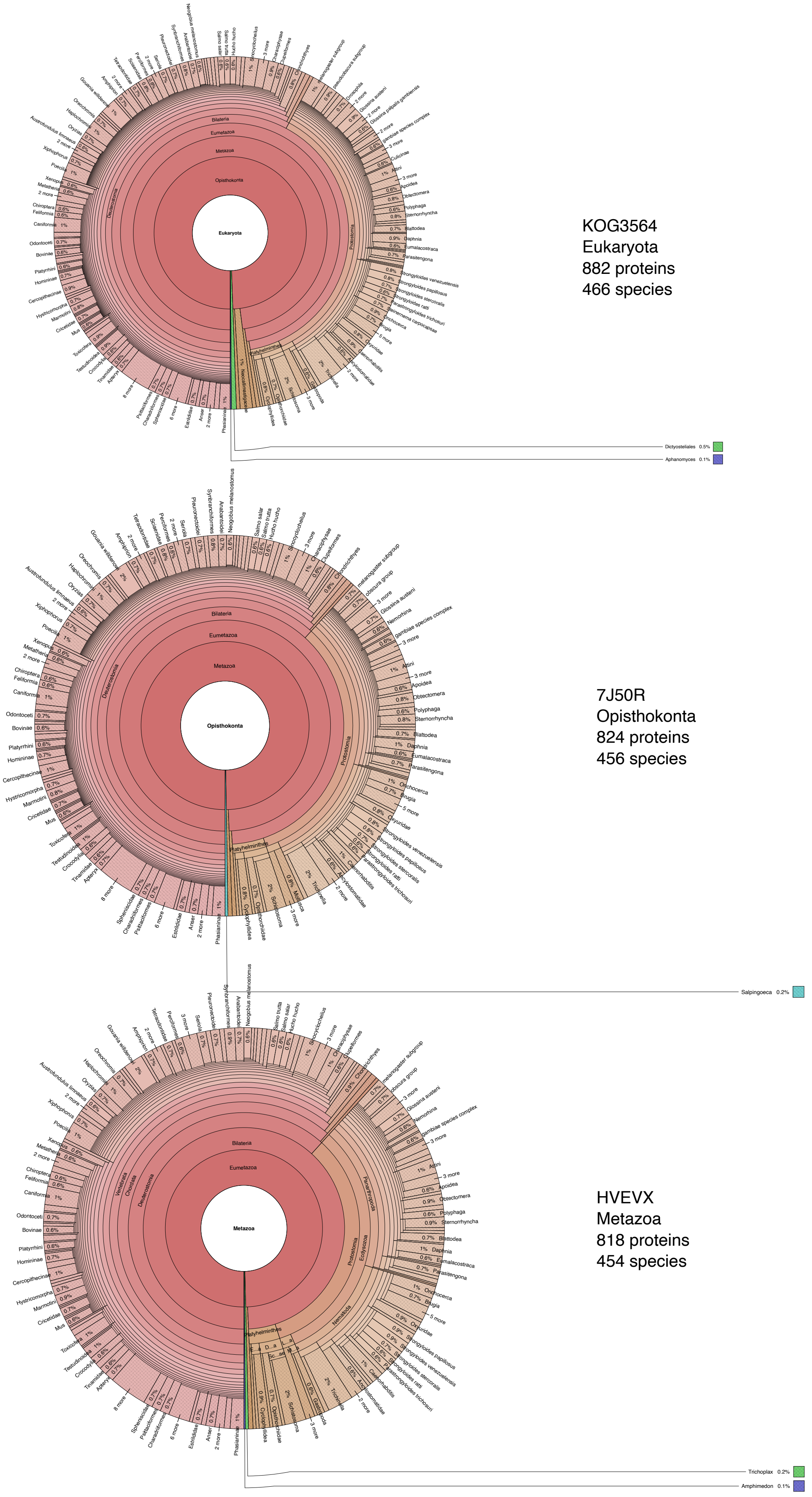

KOG3564
Eukaryota
882 proteins
466 species

7J50R
Opisthokonta
824 proteins
456 species

HVEVX
Metazoa
818 proteins
454 species

Supplemental figure 4. The taxonomic distribution of the Cyk4 unsupervised orthologous group HVEVX (bottom), the parental group 7J50R and grandparental group KOG3564. Note the number of proteins and species only increase slightly above the levels in the Metazoan OG. Source EggNOGv6.

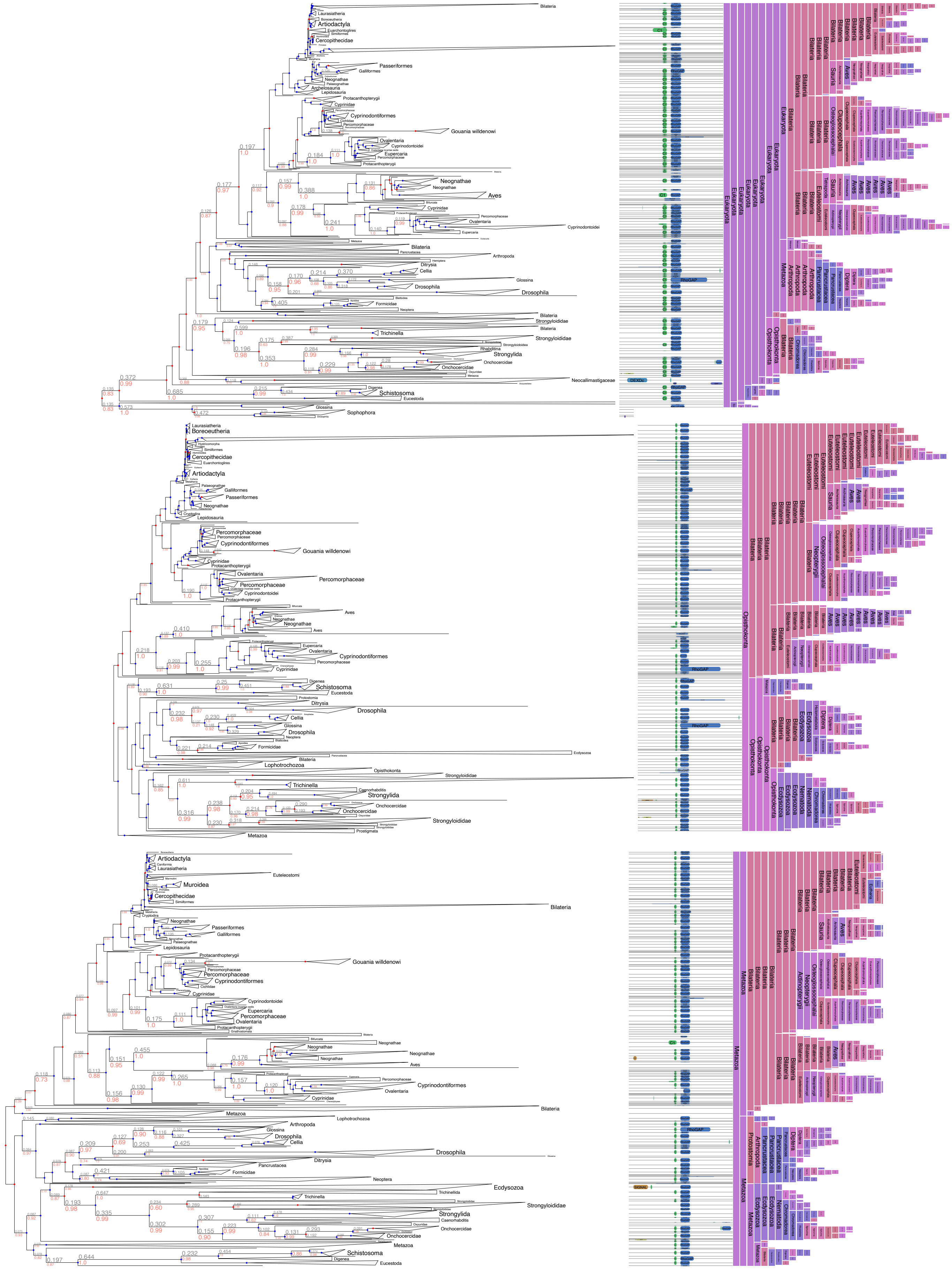
Bilateria
Laurasiatheria
Artiodactyla
Cercopithecidae
Passeriformes
Galliformes
Neognathae
Archelosauria
Lepidosauria
Protacanthopterygii
Cyprinidae
Cyprinodontiformes
Gouania willdenowi
Ovalentaria
Cyprinodontoidei
Eupercaria
Aves
Percomorphaceae
Arthropoda
Ditrysia
Cellia
Glossina
Drosophila
Formicidae
Neoptera
Strongyloididae
Trichinella
Strongylida
Onchocercidae
Neocallimastigaceae
Schistosoma
Eucestoda
Glossina
Sophophora
Boreoeutheria
Lophotrochozoa
Opisthokonta
Metazoa
Ecdysozoa
Muroidea
Euteleostomi
Pancrustacea
RhoGAP
C1
DEXDc
SIGNAL
Eukaryota
Opisthokonta
Bilateria
Metazoa
Aves
Sauria
Neopterygii
Arthropoda
Pancrustacea
Diptera
Ecdysozoa
Nematoda
Chromadorea
Protostomia

Supplemental figure 5. Taxonomic tree of the Cyk4 unsupervised orthologous group HVEVX (bottom), the parental group 7J50R (middle) and grandparental group KOG3564 (top). Note the near universal presence of the C1:RhoGAP domain (green:blue). Bars on the right indicate the last common ancestor of the corresponding proteins. Source EggNOGv6.

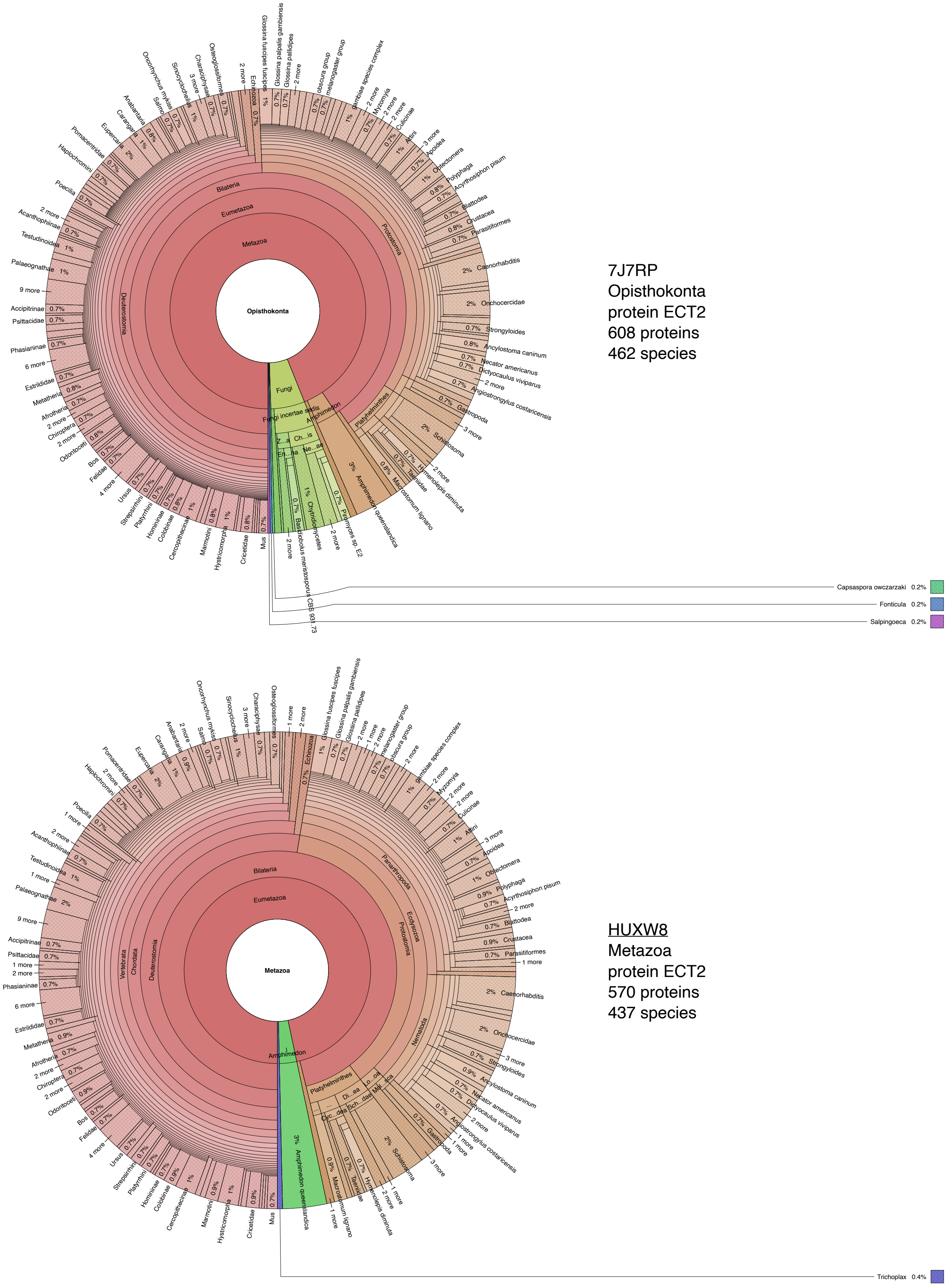

7J7RP
Opisthokonta
protein ECT2
608 proteins
462 species

HUXW8
Metazoa
protein ECT2
570 proteins
437 species

Supplemental figure 6. The taxonomic distribution of the Ect2 unsupervised orthologous group HUXW8 (bottom), the parental group 7J7RP. Note the number of proteins and species increase by < 10% in the group parental to the Metazoan OG. Source EggNOGv6.

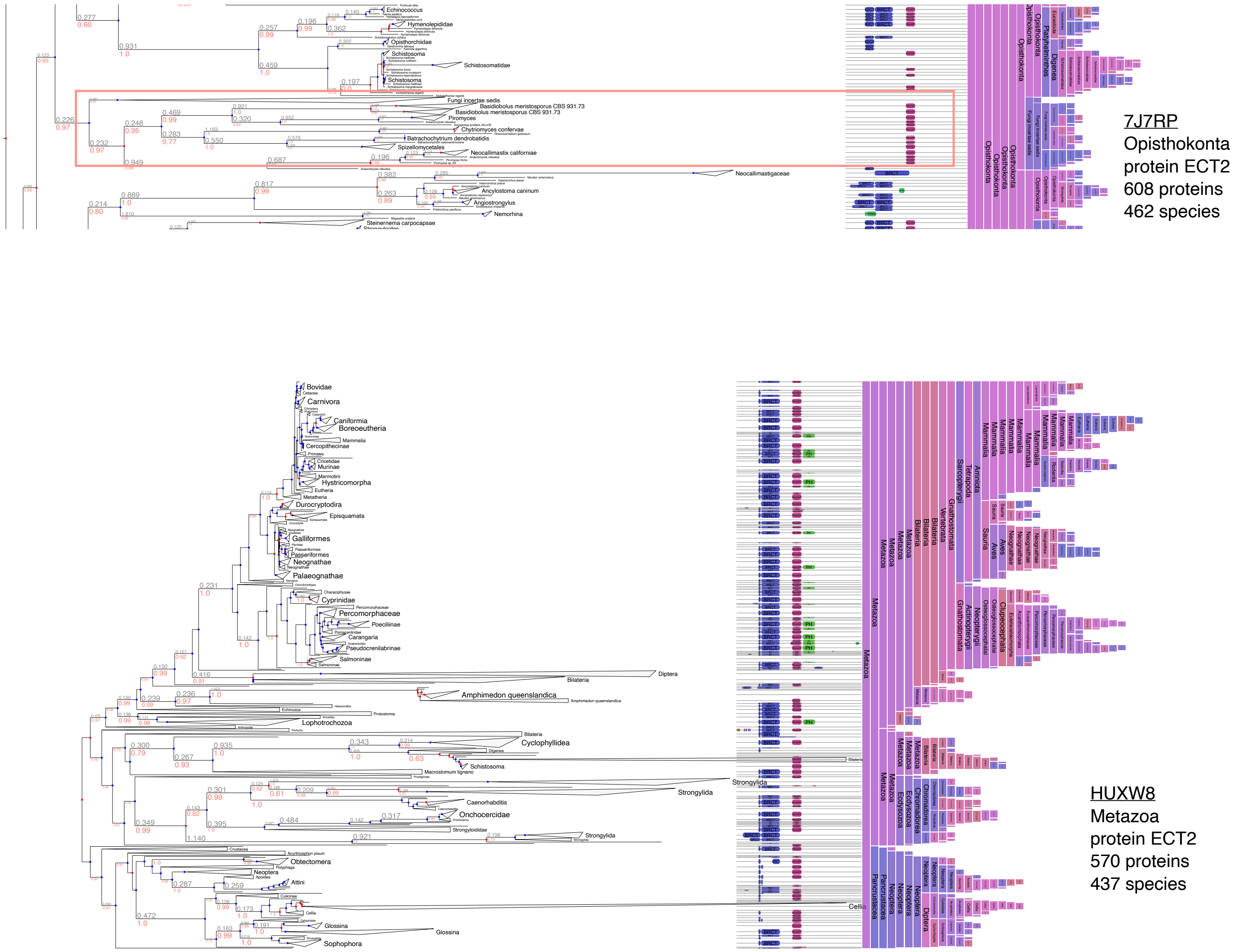
7J7RP
Opisthokonta
protein ECT2
608 proteins
462 species
HUXW8
Metazoa
protein ECT2
570 proteins
437 species

Supplemental figure 7. Taxonomic tree of the Ect2 unsupervised orthologous group HUXW8 (bottom) and a portion of the parental group 7J7RP. Note the near universal presence of two BRCT (blue) domains in Metazoa which are absent in the non metazoan species in the parental group (red box). Bars on the right indicate the last common ancestor of the corresponding proteins. Source EggNOGv6.

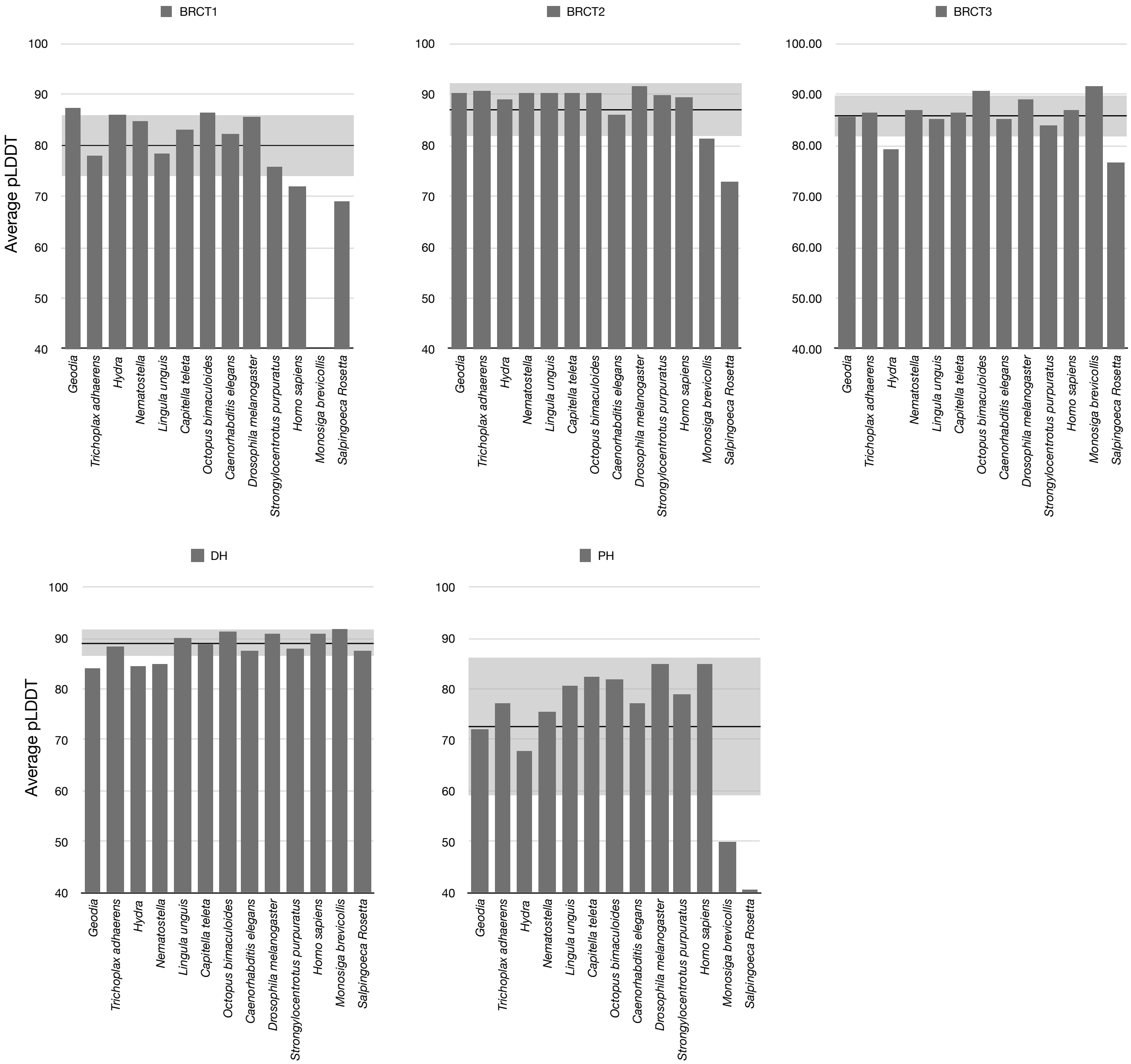

Supplemental figure 8. For each domain of the indicated proteins, the pLDDT values for each residue were extracted from the Alphafold Predictions and averaged over the domain. The line and shading represents the average +/- S.D.